

UNIVERSITY OF OKLAHOMA

GRADUATE COLLEGE

THE IMPACT OF THE MADDEN-JULIAN OSCILLATION ON EXTREME WINTER
WEATHER IN THE UNITED STATES

A THESIS

SUBMITTED TO THE GRADUATE FACULTY

in partial fulfillment of the requirements for the

Degree of

MASTER OF SCIENCE IN METEOROLOGY

By

STEPHEN FOSKEY

Norman, Oklahoma

2022

THE IMPACT OF THE MADDEN-JULIAN OSCILLATION ON EXTREME WINTER
WEATHER IN THE UNITED STATES

A THESIS APPROVED FOR THE
SCHOOL OF METEOROLOGY

BY THE COMMITTEE CONSISTING OF

Dr. Naoko Sakaeda, Chair

Dr. Jason Furtado

Dr. Jeffrey Basara

Acknowledgements

I would first like to acknowledge my advisor Dr. Naoko Sakaeda for her work in helping me write this thesis. Throughout my master's research, she has constantly provided useful feedback and guidance, and she has encouraged me when work became difficult. I would also like to acknowledge my committee members Dr. Jeffrey Basara and Dr. Jason Furtado for their work in guiding me through this thesis and providing me with feedback. And I would like to thank the fellow members of Dr. Sakaeda's research group and the Weather and Climate Interactions Group for providing me with advice on how to improve my presentations. I would like to thank my family for their support and guidance that have allowed me to get to where I am today. And I would like to thank my friends for their support and companionship as I go through this stage of my life.

Table of Contents

Acknowledgements.....	iv
Table of Contents.....	v
Abstract.....	vii
1. Introduction and Background.....	1
2. Impacts of the MJO on the Frequency of Winter Weather Events.....	9
2.1. Data and Methods.....	9
2.1.1. NCEI Storm Events Database.....	9
2.1.2. Method of Identifying MJO Impacts.....	11
2.1.3. GHCN Station Data.....	14
2.2. Climatology of Winter Precipitation.....	16
2.3. MJO Impacts on Winter Weather Frequency.....	21
2.3.1 Comparison between OMI and RMM.....	26
2.4. Lagged Frequency Ratio by OMI Phase.....	27
2.4.1 Definition of Regions.....	27
2.4.2. Frequency Ratio by Region with Lag.....	30
2.5. MJO Impacts on Precipitation and Snowfall Using Station Data.....	37
3. Physical Mechanisms Behind MJO Impacts on Winter Weather.....	41
3.1. Data and Methods.....	41
3.2. Results.....	44
3.2.1. Surface Temperature Anomalies.....	44
3.2.2. 850 hPa Temperature and Wind Anomalies.....	52
3.2.3. Geopotential Height and Wind Anomalies.....	59

3.2.4. Specific Humidity Anomalies	68
3.2.5. Large-Scale Synoptic Forcing of Ascent.....	71
4. Discussion and Conclusion.....	75
5. References	77

Abstract

Winter weather has substantial impacts on human activity, but it is challenging to predict more than 7-10 days in advance. Subseasonal-to-seasonal (S2S) prediction is a rapidly developing field of meteorology that could be used to improve winter weather prediction at longer time scales. The Madden-Julian Oscillation (MJO) is a major driver of global S2S variability. This study seeks to examine how the MJO affects the frequency of winter weather over the contiguous United States, which will help further improve winter weather prediction in the future. This is done by comparing the frequency of winter weather reports and snow accumulation data at surface meteorological stations in a given phase of the MJO to its climatology. We find that the MJO has significant impacts on increasing the frequency of extreme winter weather in the Northeast when MJO convection is in the western Indian Ocean (phase 1), the Southern Great Plains when MJO convection is in the central Indian Ocean (phase 2), and the Northern Great Plains when MJO convection is over the Maritime Continent (phase 4). These results are primarily driven by the forcing of the MJO on the jet stream and its subsequent impacts on geopotential height, as well as temperature and wind in the lower atmosphere. MJO impacts on the frequency of extreme winter weather can be seen up to 15 days in advance, suggesting utility in S2S forecasting.

1. Introduction and Background

Winter weather has significant impacts on human activity. For example, it can cause loss of life and property damage, and it can disrupt daily life over months beyond the occurrence of the initial storm (NCEI 2021a, Grundstein 2003). Therefore, it is important to be able to predict it more accurately, so people can make adequate preparations more effectively. Currently, synoptic-scale weather events like winter storms can only be predicted about 7-10 days in advance (Zhang et al. 2019), while the longer-range prediction of winter storms on subseasonal-to-seasonal (S2S) timescales remains challenging. However, recent studies have revealed that the Madden-Julian Oscillation (MJO) is one of the important drivers of global S2S variability (e.g., Jiang et al. 2020, Tseng et al. 2017, Green and Furtado 2019). The MJO is known to impact extreme precipitation and temperature over the United States (Matsueda and Takaya 2015, Zhou et al. 2012), which would likely have an impact on the frequency of winter storms as well. Therefore, to understand the potential use of the MJO as a source of S2S prediction for winter weather, this thesis will examine what impacts the MJO has on winter weather events over the United States.

The MJO is a climate mode associated with areas of enhanced and suppressed convection in the tropics, with each phase corresponding to the location of the region of enhanced convection (see Figure 1.1) (Jiang et al. 2020, Gottschalk 2014). The MJO was originally discovered as an oscillation of zonal wind in the Tropics (Madden and Julian 1971). This oscillation is further manifested by changes in patterns of convection and precipitation in equatorial regions of the globe (Jiang et al. 2020). The MJO propagates eastward at an average speed of 5 m s^{-1} (Jiang et al. 2020), and it takes 30-60 days for the main area of enhanced convection to propagate across the Eastern Hemisphere (Madden and Julian 1971). The MJO is

typically divided into 8 phases depending on where the convective activity is located (e.g., Wheeler and Hendon 2004, Kiladis et al. 2014). The areas of convection that each phase corresponds to are shown in Figure 1.1. Phase 1 of the MJO is associated with increased precipitation over the Indian Ocean. The region of increased precipitation associated with the MJO moves east to the Maritime Continent in phases 3-4, across the western Pacific in phases 5-6, and it dissipates as it moves to the central Pacific during phases 7-8. The Maritime Continent can affect the propagation of the MJO including stopping it (Jiang et al. 2020). Thus, while the MJO has substantial S2S impacts, there are also complexities that must be taken into account when it comes to forecasting the phenomenon.

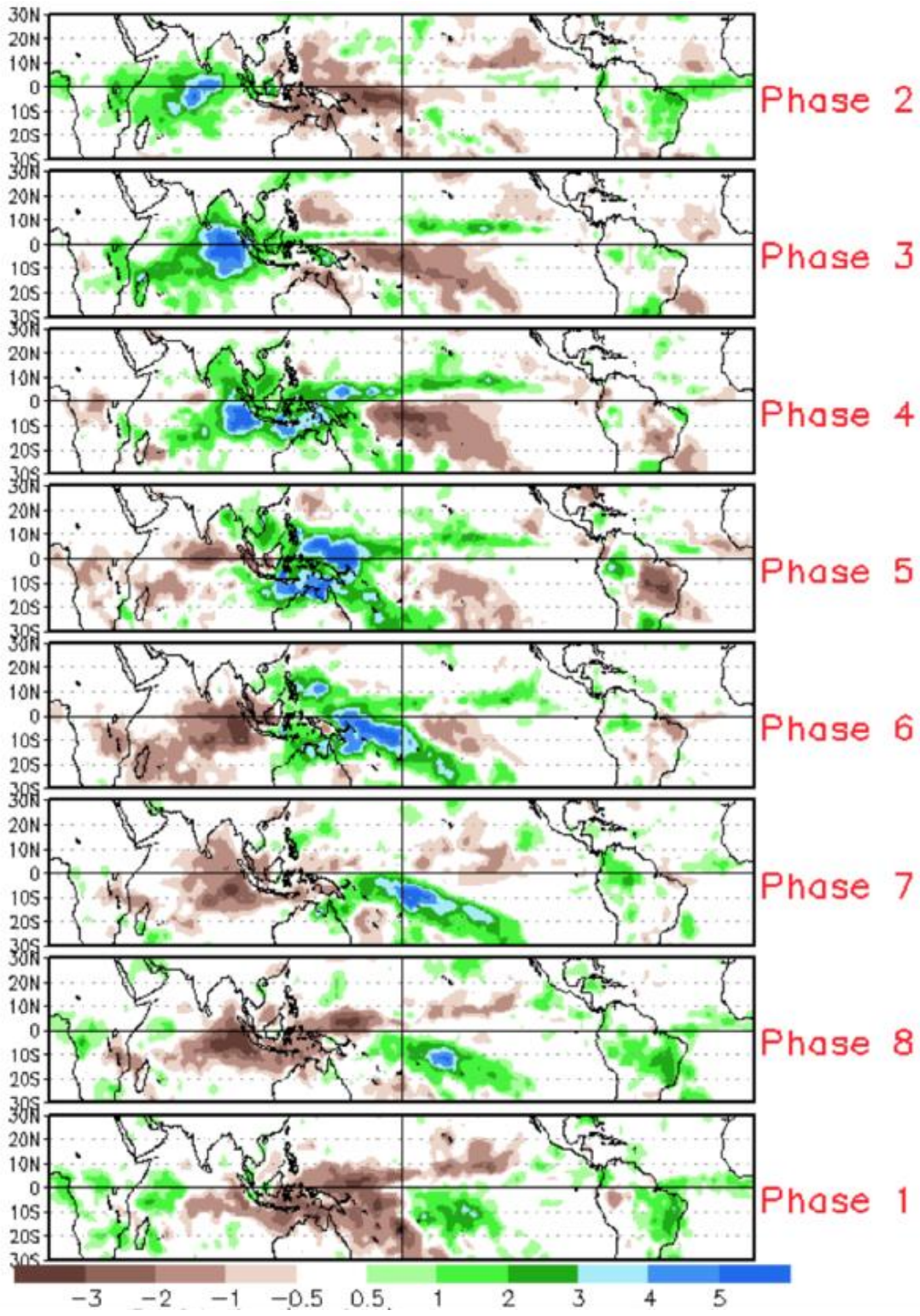


Figure 1.1: MJO precipitation by month in the Tropics. (Gottschalk 2014)

The phase of the MJO is associated with changes in wintertime temperature over much of the United States (Zhou et al. 2012). Phases 3 through 6 of the MJO tend to be associated with warmer temperatures across most of the country, while phases 8, 1, and 2 tend to be associated with cooler temperatures (Figure 1.2) (Zhou et al. 2012). Geopotential height anomalies up to 60 meters in magnitude can also be seen, with greater positive anomalies generally collocated with warmer temperatures, and vice versa (Zhou et al. 2012). These temperature anomalies can propagate in an arc from Japan, over Alaska, and into the eastern United States (Zhou et al. 2011). These correlations also apply to extreme temperatures (Matsueda and Takaya 2015).

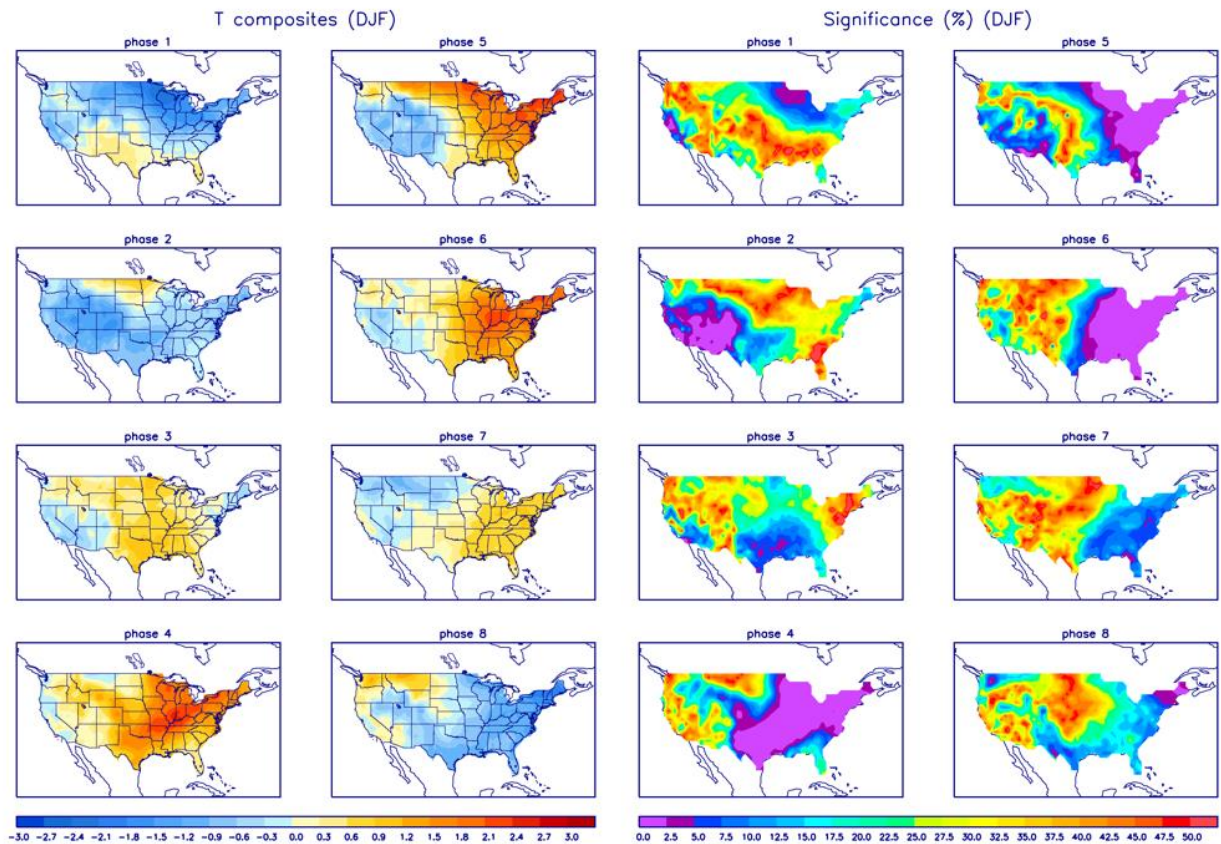


Figure 1.2: Temperature anomalies ($^{\circ}\text{C}$) associated with the MJO during the months of DJF.

(Zhou et al. 2012)

These geopotential height and temperature anomalies associated with the MJO may help form the synoptic conditions that can lead to extreme winter weather, which can differ based on the region of the country where the event occurs. Correlations have been found between the MJO phase and snowfall over southeastern New England (Klotzbach et al. 2016). The authors found decreased snowfall in phases 4-6, and increased snowfall in phase 7 (Klotzbach et al. 2016). They attributed the increased snowfall in phase 7 to cyclonic wave breaking in the region (Klotzbach et al. 2016). However, the impact of the MJO on winter weather over other regions is not well understood. In the Southern Great Plains, winter storms often have a shortwave trough to the west and a jet streak to the east, with snow occurring more frequently towards the northwest and ice occurring along a line extending from the southwest to the northeast (Mullens et al. 2016). Low pressure systems causing heavy snow and blizzards over the Northern Plains often originate in Colorado or Alberta, and track eastward (Black 1971). Winters with higher snow water equivalent in the Northern Plains tended to have more troughing over the United States, while winters with lower snow water equivalent tended to have ridging (Grundstein 2003). These studies show that the location of synoptic low-pressure centers influences where winter weather events are likely to occur. Therefore, the MJO will likely impact the frequency of winter weather events over different regions throughout its lifecycle as it modulates the preferred location of anomalously low geopotential height and surface pressure over the United States.

Different dynamical and physical processes are believed to cause the MJO to have extratropical impacts. Sardeshmukh and Hoskins (1988) found that the advection of vorticity by irrotational flow was one way in which the tropics could influence the extratropics. While a Rossby wave source is important, that source is actually located near the subtropical jet and not the equator (Sardeshmukh and Hoskins 1988). Green and Furtado (2019) also found that the

MJO, in combination with the strength of the stratospheric polar vortex, could be used to predict temperature over the United States. Either a weak stratospheric polar vortex or the MJO in phases 7 and 8 tend to lead to increased blocking and decreased geopotential height over the eastern United States (Green and Furtado 2019). However, the combination of the two leads to moderate to slightly increased geopotential height over the southeastern United States (Green and Furtado 2019). The thermal impacts of the MJO can be felt as far north as the Arctic, and could be caused by temperature or moisture advection (Vecchi and Bond 2004). Warmer temperatures over the Arctic, as measured by 500 hPa geopotential height, are correlated with increased winter storm severity over the United States (Cohen et al. 2018). Given the MJO impacts on temperatures over the United States can happen due to a Rossby wave train propagating across Alaska (Zhou et al. 2011), it seems reasonable to consider the polar regions when making an account of possible impacts of the MJO on the mid-latitudes.

The MJO may also impact winter weather over the United States indirectly by influencing the North Atlantic Oscillation (NAO). The NAO is an oscillation of sea-level pressure between Iceland and the Azores (Greatbatch 2000), which can influence temperature and winter weather over the United States (Greatbatch 2000, Hartley and Keables 1998). A positive phase has a stronger Icelandic low and a stronger Azores high, while a negative phase has a weaker pressure differential (Greatbatch 2000). A negative NAO tends to lead to more blocking over eastern North America and western Europe, while a positive NAO has the opposite effect (Greatbatch 2000). This means a negative NAO can lead to colder temperatures and more winter weather events over the aforementioned regions (Greatbatch 2000). Some studies have already found a correlation between each pairing of the MJO, the NAO, and temperatures over the United States (e.g., Lin et al. 2009, Cassou 2008). They have analyzed

these relationships both instantaneously and with a lag between the two phenomena. Lin et al. (2009) noted that phase 3 of the MJO tended to result in a positive phase of the NAO about five days later, whereas phase 7 usually resulted in a negative NAO phase. Cassou (2008) found that the phase of the MJO had an influence on the phase of the NAO over the course of about 12 days. They attributed the MJO's influence on the NAO to be caused by anticyclonic wave breaking (Cassou 2008). They found a four-part cycle of pressure variation in the North Atlantic and Northern Europe. Cassou (2008) found that the MJO drives a positive NAO, and then the rest of the NAO cycle proceeds from there. After the MJO drives the positive phase of the NAO, the 500 hPa height pattern progresses to a Scandinavian blocking pattern. Then the cycle proceeds to the negative phase of the NAO. The last part of the cycle is the Atlantic ridge pattern. The connections between the MJO and the NAO were shown to affect the patterns of precipitation and snowfall over the Mid-Atlantic of the United States during the 2009-10 winter (Moon et al. 2012). Thus, this analysis will look not just at the Tropics and the United States, but the entire Northern Hemisphere.

The MJO and NAO both influence teleconnections, which are patterns in atmospheric variables that occur across broad regions. Many such patterns have been found, particularly over the Northern Hemisphere (Wallace and Gutzler 1981). Teleconnections are often believed to be useful for predicting longer range environmental patterns. For example, the MJO can increase predictability at periods of about two to three weeks (Tseng et al. 2017). This predictability in the European Centre for Medium-Range Weather Forecasts (ECMWF) model is stronger when the MJO is in phases 1, 2, 5, and 6 (Tseng et al. 2017). The MJO even has a statistically significant correlation with 500 hPa geopotential height after a lag of one month from the MJO being in phase 3 (Tseng et al. 2017). This is due to the MJO influencing the Pacific North America

Pattern (PNA), which then influences global patterns (Tseng et al. 2017). Thus, the MJO plays an important role when it comes to S2S forecasting. Some authors have also looked at teleconnection patterns over longer time scales (e.g., Riddle et al. 2013) and how these patterns can influence winter weather over the United States (e.g., Serreze et al. 1998).

The goal of this thesis is to determine the atmospheric patterns that are favorable for winter weather at long range, with the hope that this will improve predictability of extreme winter weather. This will be done by determining the impacts of the MJO on the frequency of extreme winter weather over the contiguous United States. The ways the MJO impacts the frequency of extreme winter weather will be determined by comparing the influence of the MJO on patterns of atmospheric variables such as temperature, wind, and moisture to those patterns during days where extreme winter weather occurs. These patterns will also be compared to the NAO and PNA. Based on this information, we hypothesize that the frequency of extreme winter weather is influenced by the phase of the MJO in that it is affected by Rossby wave propagation out of the tropics, with troughing and resultant cooler temperatures and increased moisture over parts of the United States in certain phases. This hypothesis will be tested in the upcoming sections.

2. Impacts of the MJO on the Frequency of Winter Weather Events

This section will first determine if and where the MJO influences the frequency of winter weather events over the contiguous United States. Then it will determine if these influences are found with a lag of several days after a given MJO phase. This is the first time a study has examined the impacts of the MJO on winter weather over the entire CONUS. The potential influence of the MJO on winter weather will be examined by analyzing how the frequency of winter weather events relative to climatology changes in each phase of the MJO.

2.1. Data and Methods

2.1.1. NCEI Storm Events Database

The frequency of winter weather events is estimated using the National Centers for Environmental Information (NCEI) Storm Events Database (Storm Database) (NCEI 2021a), which contains reports of impactful weather events across the country grouped into different categories. This database has winter weather reports going from 1996 to the present. However, 2018 was chosen as the final year of the analysis for this project. That is because the data can be modified up to 18 months after a given event, and the project started in 2020. So, 2018 was the latest finalized year of data when the project started. Three categories of reports were analyzed: ice storms, winter storms, and heavy snow. An ice storm report is made when a weather event meets the National Weather Service (NWS) warning criteria for ice accumulation, a winter storm report is made when an event meets warning criteria for ice, sleet, and/or snow accumulation, and heavy snow is reported when an event meets warning criteria for snow accumulation (Table 2.1). Only the months of December through March are analyzed in this study, after a preliminary climatological analysis showed that those months had approximately 85% of all storm reports.

This is also done to limit the influence of the seasonal variability of the MJO (Wang and Xie 1997, Wheeler and Hendon 2004) on the results.

Table 2.1: NWS criteria for given storm types.

Ice Storm	Heavy Snow	Winter Storm
Ice accretion exceeding locally defined warning criteria	Snow accumulation exceeding locally defined warning criteria	Winter weather event with multiple significant hazards
Usually at least 0.25-0.5” (6.3-12.5 mm) of ice	Usually at least 4-10” (10-25 cm) of snow	At least 0.25-0.5” (6.3-12.5 mm) of freezing rain, 4-10” (10-25 cm) of snow, and/or 1-2” (2.5-5 cm) of sleet
No sleet or snow	No freezing rain or sleet	Some combination of snow, sleet, freezing rain, and blowing snow

Storm report data are also cataloged by zone, where a zone is a geographical area defined by the NWS that is used to issue watches and warnings. A given zone is typically a county or part of a county, and has an average area of 1874 km² (Huguley 2009). This is much smaller than the size of a typical winter storm, so any given zone is very unlikely to have multiple winter storms at the same time. Furthermore, zones usually cover areas with similar climatic conditions. Thus, a winter storm will typically produce a similar type of weather across the entire zone. If a zone has a winter storm report, the entire zone likely had winter weather, so the number of zones with storm reports is a good proxy for the area covered by a given winter storm.

A December-March (DJFM) climatology of winter weather report frequency is created to determine in which areas of the country different types of winter weather are most frequent. This would be useful when later analyzing the magnitudes of the impacts and the sample size of the results. It would also be useful in determining which areas to focus on for further analysis. To calculate the climatology, the number of days with each type of weather report is examined by state and then by NWS weather forecast office (WFO) county warning area (CWA). To examine the frequency of winter weather reports, a method to normalize the number of winter weather reports in each WFO or state must be introduced to account for differences in the area. A WFO with a larger area has a greater number of zones. Therefore, a WFO with a higher number of zones will likely have a larger number of reports from one weather system, as a given system will likely pass over multiple zones. For that reason, the average annual count of reports in each state or WFO is normalized by the number of zones in the region to give an average annual frequency of winter weather reports per zone in the region.

$$\text{annual frequency} = \frac{N_{reports}}{N_{years} \times N_{zones}}$$

Equation 2.1: Definition of annual climatological frequency, where $N_{reports}$ is the number of storm reports in a given state or CWA, N_{years} is the number of years in the dataset, and N_{zones} is the number of zones in the state or CWA.

2.1.2. Method of Identifying MJO Impacts

After the climatology is computed, we examine how the frequency of winter weather events changes with the phase of the MJO. From the NCEI data, the average number of daily reports of each given storm type in a given MJO phase is compared to the climatological

frequency of reports of that storm type, which will be referred to as a frequency ratio (Equation 2.2). This ratio provides the increased or decreased likelihood of extreme winter weather in a given MJO phase relative to climatology. Given that the definition of winter weather reports is subjective and depends on each WFO, this normalization eliminates those caveats.

$$\textit{frequency ratio} = \frac{\textit{frequency of storms per MJO phase}}{\textit{climatological frequency}}$$

Equation 2.2: Definition of frequency ratio, where the frequency of storms per MJO phase and climatological frequency are daily frequencies.

Frequency ratios greater than 1 imply an event occurs more frequently than climatology, while frequency ratios less than 1 imply an event occurs less frequently than climatology.

A frequency ratio of 2 means an event occurs twice as often as climatology, and a frequency ratio of 0.6 means an event occurs 60% as often as climatology, for example. WFOs with no events in any phase were not considered for analysis.

Frequency ratio was examined for each phase of the MJO, determined by both the Outgoing Longwave Radiation (OLR) MJO Index (OMI) (Kiladis et al. 2014) and Real-time MJO Monitoring Index (RMM) (Wheeler and Hendon 2004). These phases are calculated using empirical orthogonal function (EOF) analysis with the first two principal components found. The values of the principal components are plotted on a phase diagram. The data going into the EOFs can include OLR and zonal winds at 850 hPa and 200 hPa over the tropics. The areas of negative OLR are areas of convection. The RMM includes zonal winds while the OMI does not. We present the results using the OMI for the majority of this analysis, but we also discuss the sensitivity of the results to the choice of indices. Because the OMI ignores variations in wind not

associated with the MJO, it can more accurately identify the location and magnitude of the MJO convective signal (Straub 2013). The OMI also applies 20-96-day bandpass filtering, which removes the effects of Kelvin waves, so the OMI picks up a signal more strongly associated with the MJO (Kiladis et al. 2014). This is especially helpful when diagnosing the causes of the influence of the MJO on the frequency on winter weather done in Chapter 3. The OMI was found to have similar dates with given phases as compared to the RMM. This is in agreement with the results of Kiladis et al. (2014). We have also examined the frequency of storm reports during periods of weak or no MJO, which was determined by an amplitude less than 1 standard deviation (0.6321 in DJFM) for OMI, and an amplitude less than 1 for RMM. This is because it is plausible the lack of MJO convection could be important for winter storm development.

The results are tested for statistical significance using a bootstrapping method with 1000 iterations. A random subset of the days of each MJO phase was resampled with replacement for each iteration. A one-tailed 90% significance level is used. This means that a given phase had a statistically significant frequency ratio if 90% of the resampled sets of days had a frequency ratio greater than 1. We did not test if a frequency ratio is statistically significantly less than one (i.e., less frequent than climatology). However, percentile values were recorded to get a sense of the level of significance of each result. One tailed sampling is used because phases with increased risk of extreme winter weather events would be more societally impactful. So, it is important to focus on those regions and phases. Other sampling methods involved two-tailed tests or a 95% significance level, both of which produced similar results. Monte Carlo sampling (i.e., sampling over all days as opposed to resampling days with a given MJO phase) also produced similar areas of significant frequency ratios.

Similar to the climatology, these data are organized with events grouped first by state and then by county warning areas (CWAs) of NWS Weather Forecast Offices (WFOs). WFOs are chosen for the final analysis because the warning thresholds vary by WFO; thus, there is consistency within each office's CWA. This did reduce the sample size somewhat because there are 48 states in the contiguous US, but 118 WFOs. However, use of WFO CWAs allowed finer-scale geographical variation to be more visible.

If we work under the hypothesis that the MJO influences winter weather over the United States via the propagation of Rossby waves, it is important to note that it will take several days for those Rossby waves to propagate from the Tropics to the U.S. (Riddle et al. 2013). So, frequency ratio was also analyzed with a lag of five, ten, and fifteen days. These lag times were chosen because each MJO phase lasts approximately five days (Tseng et al. 2017). The results show how the MJO could influence winter weather over time. Data were also analyzed over selected regions with regard to phase and lag, to determine if the frequency ratio still varied as much as 15 days after a given MJO phase.

2.1.3. GHCN Station Data

While the NCEI Storm Database provides the frequency of different winter weather events, those events are subjectively defined at each WFO. To ensure that our results are robust to this caveat of the Storm Database, we also analyzed precipitation and snowfall data from the Global Historical Climatology Network (GHCN) (NCEI 2021b). In this dataset, sleet is counted as snow. GHCN data exist for over 100,000 stations around the world from various observing networks, including the Automated Surface Observing System often found at airports, co-op stations, and data from sources such as the High Plains Regional Climate Center and Western

Regional Climate Center (NCEI 2021b). These data go back as far as 1833, and include records of maximum and minimum temperature, precipitation, and snowfall (NCEI 2022). Use of GHCN data allowed a longer period of record, as many stations have data going back before the start of MJO data in 1979. Out of 1218 stations with data, 846 had sufficient precipitation data, and 777 had sufficient snow data. Sufficient precipitation data was defined as at least 85% of days with non-missing precipitation data, and sufficient snow data was defined as at least 60% of days with non-missing snow data. These thresholds were somewhat subjective, as we sought to achieve a balance between sample size and accurate data. For example, if the precipitation threshold was raised to 90%, the number of stations with precipitation data fell to around 600. The snow threshold was chosen to be lower than the precipitation threshold because many stations have more missing snow data. Impacts of the MJO on snowfall were not analyzed for stations with no snow accumulations during the entire time period. Since data were recorded by total precipitation or snowfall accumulation, the impact of the MJO on GHCN precipitation and snowfall was examined by the ratio of daily average precipitation and snowfall accumulation in a given OMI phase to their climatological average values (i.e., accumulation ratio). Values greater than 1 indicate accumulation greater than climatology, and values less than 1 indicate accumulation less than climatology. The relatively large number of stations compared to WFOs allowed finer resolution in the results. And since most snow events during the time period were recorded, instead of just the larger ones as in NCEI, the sample size of events was larger. This resulted in larger regions of significant accumulation ratios. Significance was determined with bootstrapping in the same manner as the Storm Database.

2.2. Climatology of Winter Precipitation

Climatology of Winter Weather Events

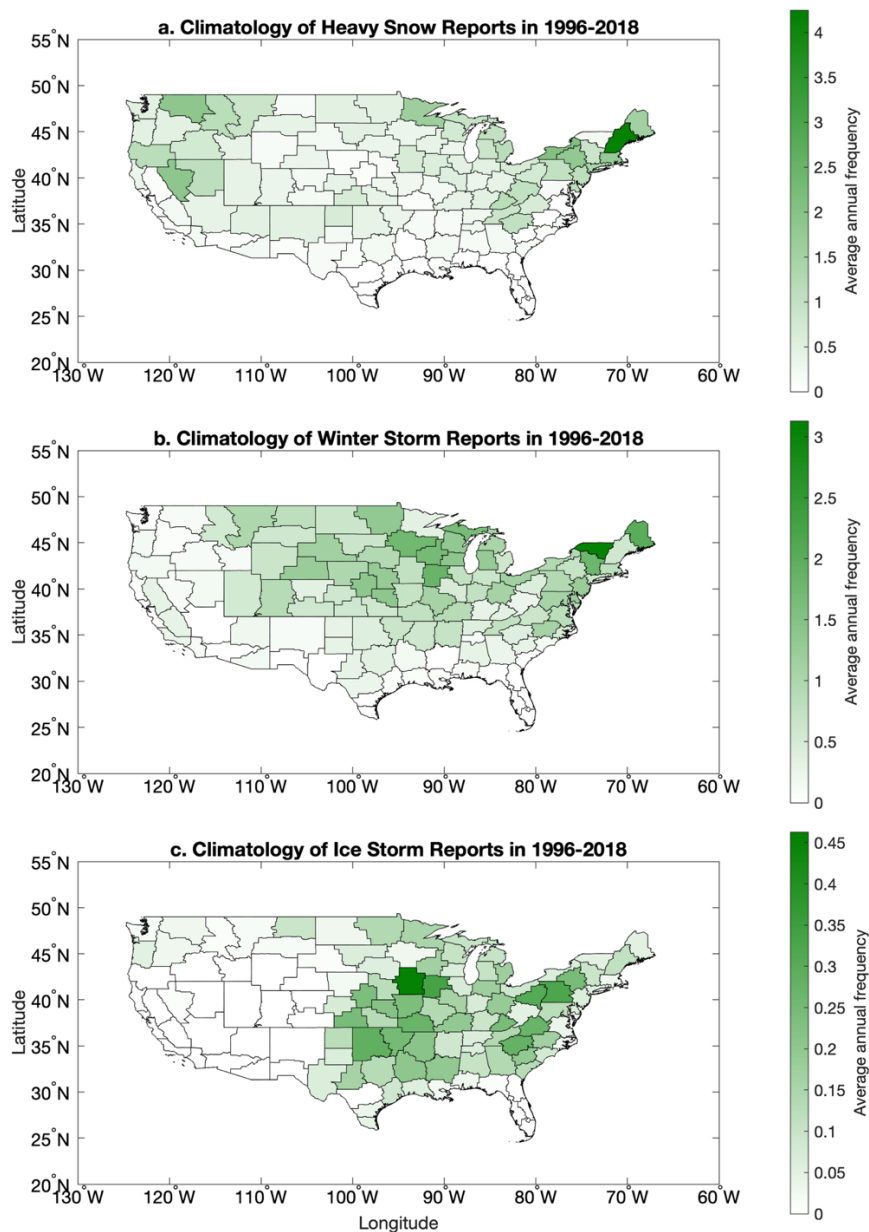


Figure 2.1: Climatology of winter weather reports from 1996-2018 in average number of reports per year per zone in each WFO county warning area for a. ice storms, b. winter storms, and c. heavy snow, all as defined in the NCEI storm event database.

Heavy snow events tend to be most frequent over the Northeast and Northwest United States (Figure 2.1a). Some other regions with frequent heavy snow events include the Sierra Nevada and Appalachian Mountains. These areas tend to have cold temperatures conducive to precipitation events being all snow, and more precipitation than the Northern Plains region of the United States (Changnon 2006).

Winter storms are most frequent in the Northeast U.S. (Figure 2.1b). This region of the country experiences frequent nor'easters, which often feature changing precipitation types as the low pressure moves to the northeast (Zielinski 2002). The maximum frequency here is around 3 per year. There is a secondary maximum of around 2 winter storms per year over the western Great Lakes region. This part of the country is also often along the rain/snow line in winter, and is west of the lake effect snow region downwind of the Great Lakes (Wiley and Mercer 2021). The highest frequency of winter storms is in the Burlington, Vermont area at just over 3 reports per year, while the highest frequency of heavy snow events is over the Gray, Maine area. However, Gray has a much lower frequency of winter storms, and Burlington has a much lower frequency of heavy snow reports. Given that both areas experience similar weather patterns, this discrepancy is likely due to how individual offices categorize winter weather events. As an example, on 12 January 1996, both WFOs received widespread reports of 6-12" (15-30 cm) of snow, but it was counted as a winter storm in Burlington and heavy snow in Gray. However, this work is only comparing differences with regard to a local office's climatology, so discrepancies between offices should not have a major impact on the results.

Ice storms are most frequent over the central and eastern United States (Figure 2.1c). This region frequently has temperature inversions due to phenomena such as cold air damming or

precipitation ahead of a warm front (Changnon and Karl 2003). The maxima over the central US and the Appalachians are similar to those found in climatologies (e.g., Changnon and Karl 2003). However, NCEI reports are lower in the Northeast relative to other areas of the country, while freezing rain is relatively more common there (Changnon and Karl 2003). This is likely because the Northeast is more prone to short-duration freezing rain events, that often result in lesser accumulations than in the central US (McCray et al. 2019). The maximum frequency of ice storms in the NCEI database is only around 0.45 reports per year over central Iowa. This is because many events colloquially referred to as ice storms also feature significant amounts of sleet and snow, which means the storms would instead be classified as winter storms in NCEI.

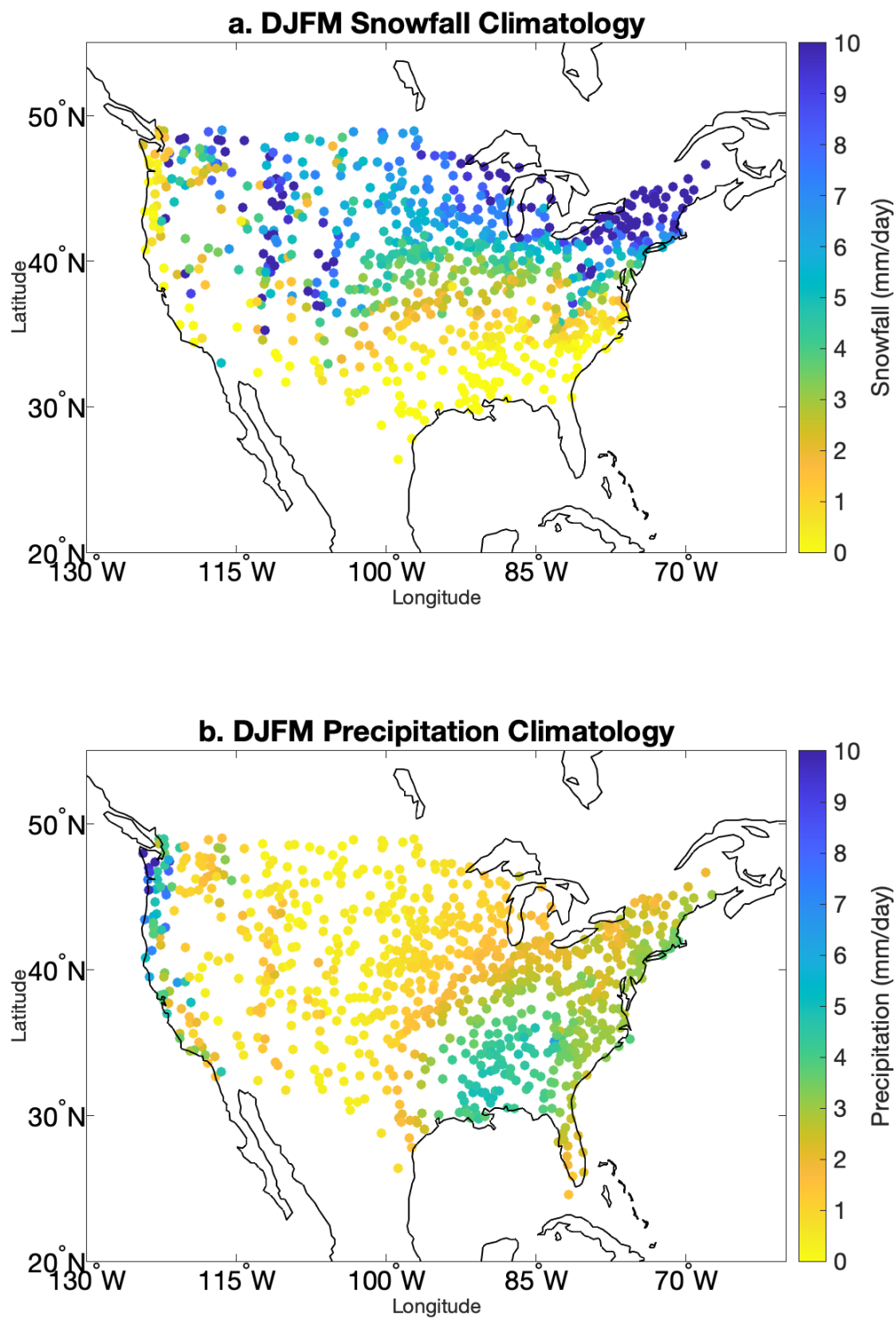


Figure 2.2: Climatology of mean daily a. snowfall and b. precipitation in DJFM based on the GHCN dataset. Note that snowfall is measured in total accumulation and not liquid equivalent, so snowfall values may be greater than precipitation values.

The GHCN snow accumulation climatology (Figure 2.2a) has similar maxima as the NCEI heavy snow report climatology. Both climatologies feature maxima in the interior Northeast, Great Lakes, and Mountain West regions. However, the precipitation climatology looks quite different (Figure 2.2b). There is a maximum of over 10 mm/day along the coast of Washington, and a secondary maximum of around 6 mm/day over the interior South. There is also a slight precipitation maximum along the east coast. The North Central U.S. has high snow values and low precipitation values. This is because cold temperatures lead to precipitation being mostly snow, and can cause higher snow to liquid ratios.

2.3. MJO Impacts on Winter Weather Frequency

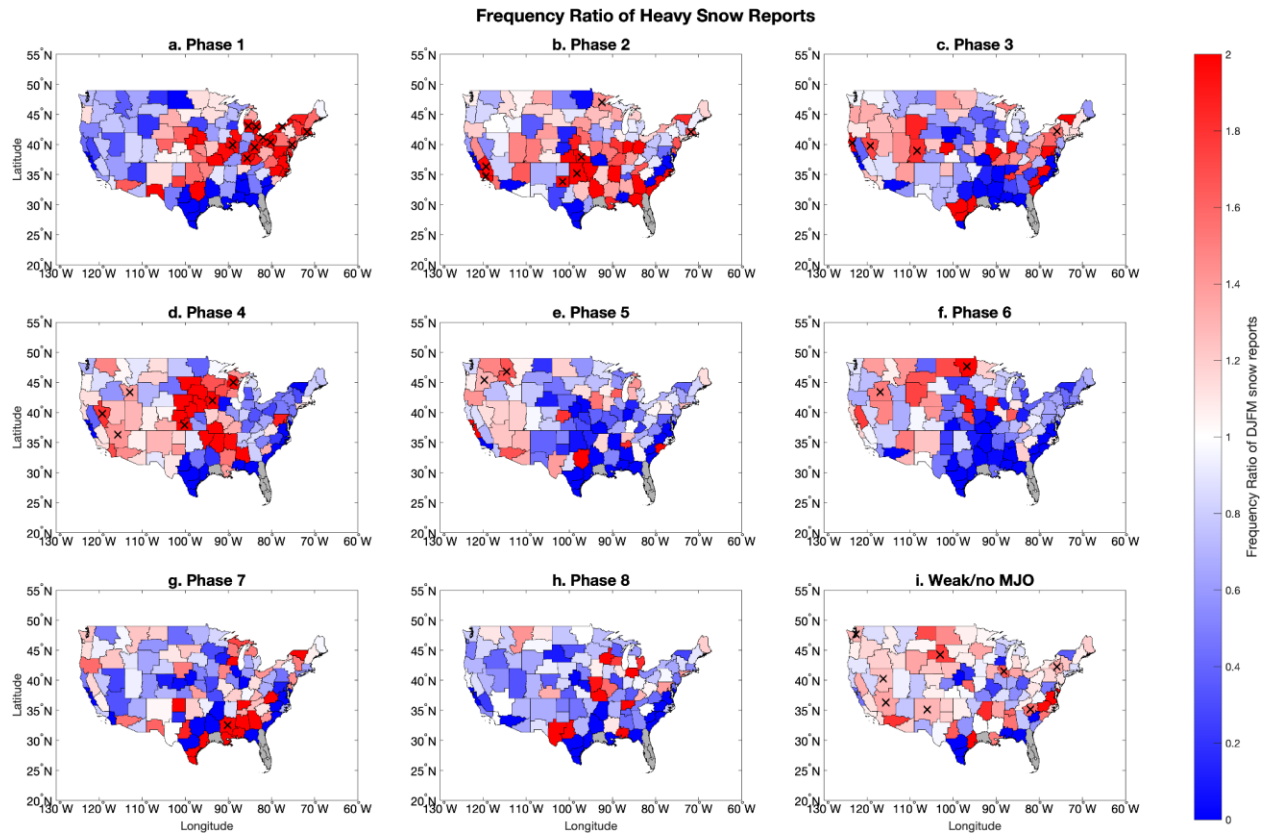


Figure 2.3: Frequency ratio of heavy snowfall reports over the United States by OMI phase. The X marks statistical significance for values greater than 1 at the 90% confidence level. Gray areas had no heavy snow events in the WFO during the study period. Values greater than 2 are also plotted in red.

As can be seen in Figure 2.3, there are significant variations in heavy snow frequency by OMI phase. In phase 1, the area of highest frequency is located in the Northeast, with many areas receiving heavy snow twice as frequently as the climatological average. Phase 1 also produced the greatest number of statistically significant regions. In phase 2, the areas of greatest frequency ratio shift to the Southern Plains. In phase 3 the highest frequency ratios shift toward the West Coast. Phase 4 has high frequency ratios in the central and western United States, while it shifts

to the Pacific Northwest in phase 5. Phase 6 has the highest values in the far Northern Plains, while in phase 7 it is in the Deep South. Phase 8 does not have any regions of significantly higher than normal frequency of heavy snow events. Phases 5-8 have generally lower frequency ratios across the country. While significance was not plotted for low frequency ratios, many bootstrapped frequency ratio values were below the mean over 95% of the time. Therefore, some of these below-normal frequency ratios are quite anomalous. Most regions only have a high frequency ratio in one or two phases.

The patterns are approximately cyclic, with areas of high frequency ratios often having lower frequency ratios four phases later. However, this pattern does not apply to all regions; for example, northern New England has high frequency ratios in phases 3 and 7. A lot of the irregularities in this variation are likely due to noise. Yet there are clear conglomerations in areas of higher or lower frequency ratio, like the area of over 1.5 frequency ratios in phase 4 that stretches from Wisconsin to western Kansas, and continuous values greater than 1 as far west as the Sierra Nevada. All but two of the CWAs in that region have frequency ratios less than 1 in phase 8. Florida and southwest Louisiana did not record any heavy snow events during the time period. Yet in spite of lower sample sizes in the South, the Jackson, Mississippi WFO featured a significant frequency ratio of double the climatology in phase 7.

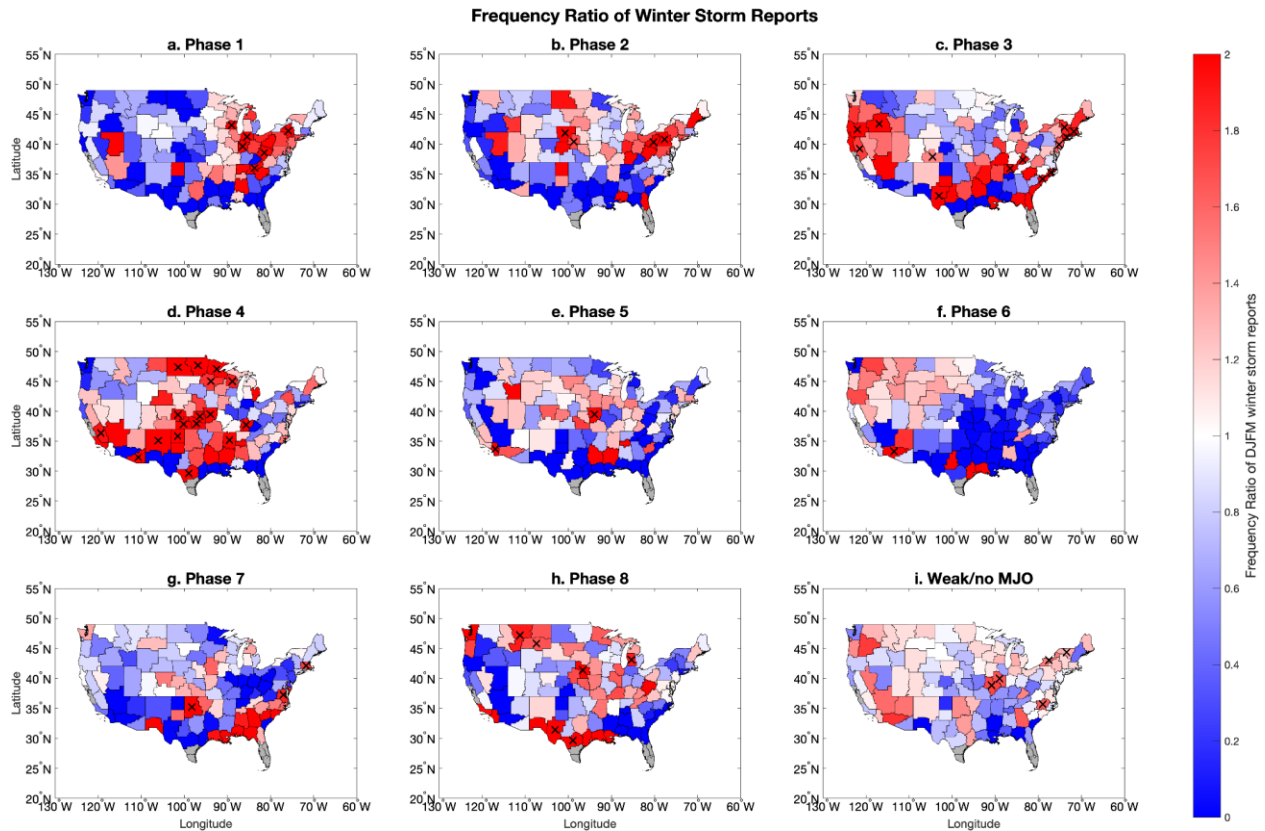


Figure 2.4: Same as Fig. 2.3 except showing the frequency ratio of winter storm reports.

The frequency ratios for winter storms (Figure 2.4) are similar to those for heavy snow events. The greatest frequency ratios start in the Northeast in phase 1, shift west by phase 3, peak in the Great Plains by phase 4, and are generally lower in phases 5 through 8. However, phase 8 has somewhat higher frequency ratios for winter storms as compared to heavy snow events. Additionally, the areas where the MJO has a significant impact in the Great Plains during phase 4 are much larger for winter storms compared to heavy snowfalls. Phases 2 and 3 also have a greater frequency of winter storm reports in the Northeast as compared to heavy snow, while the opposite was true for phase 1.

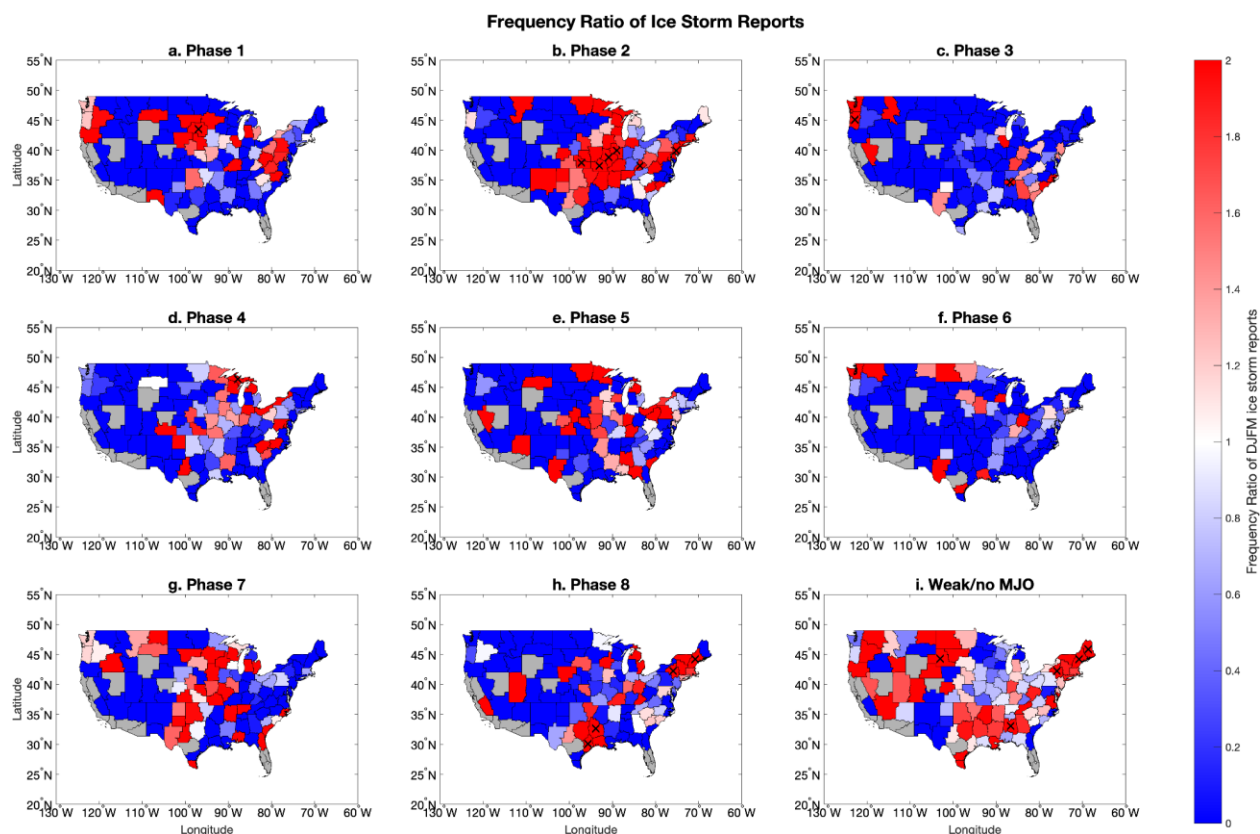


Figure 2.5: Same as Fig. 2.3 except showing the frequency ratio of ice storm reports.

For ice storms, the areas of significant MJO impact were much smaller, due to the smaller frequency of ice storm events nationwide (Figure 2.5). The data appear noisier for the same reason. This is particularly true over the western United States, where many CWAs did not report a single ice storm during the time period. However, the MJO has significant impacts on the frequency of ice storms over some regions. For example, phase 2 has an area of high frequency ratios in the Central Plains, similar to winter storms and heavy snow. Phase 8 also has areas of significant high frequency ratios around Texas/Louisiana and in the Northeast. One thing to note with all of these results is that there are areas of significant large frequency ratios even for times of weak or no MJO. This suggests that even a lack of MJO could provide some information to forecasters about the likelihood of severe winter weather.

When comparing frequency ratios using state boundaries versus CWA boundaries (not shown), the results tended to be similar, both in terms of frequency ratio and areas of significance. This was the case for each phase and storm type (not shown). This suggests that the broader patterns of MJO influence on winter weather frequency are not very sensitive to the type of region used to group reports, be it state or CWA boundaries. The maps with CWA boundaries do tend to be a bit noisier due to the smaller sample size, but also group regions with the same criteria for severe winter weather. Thus, those regions are insensitive to the definitions of how each WFO classifies severe winter weather.

2.3.1 Comparison between OMI and RMM

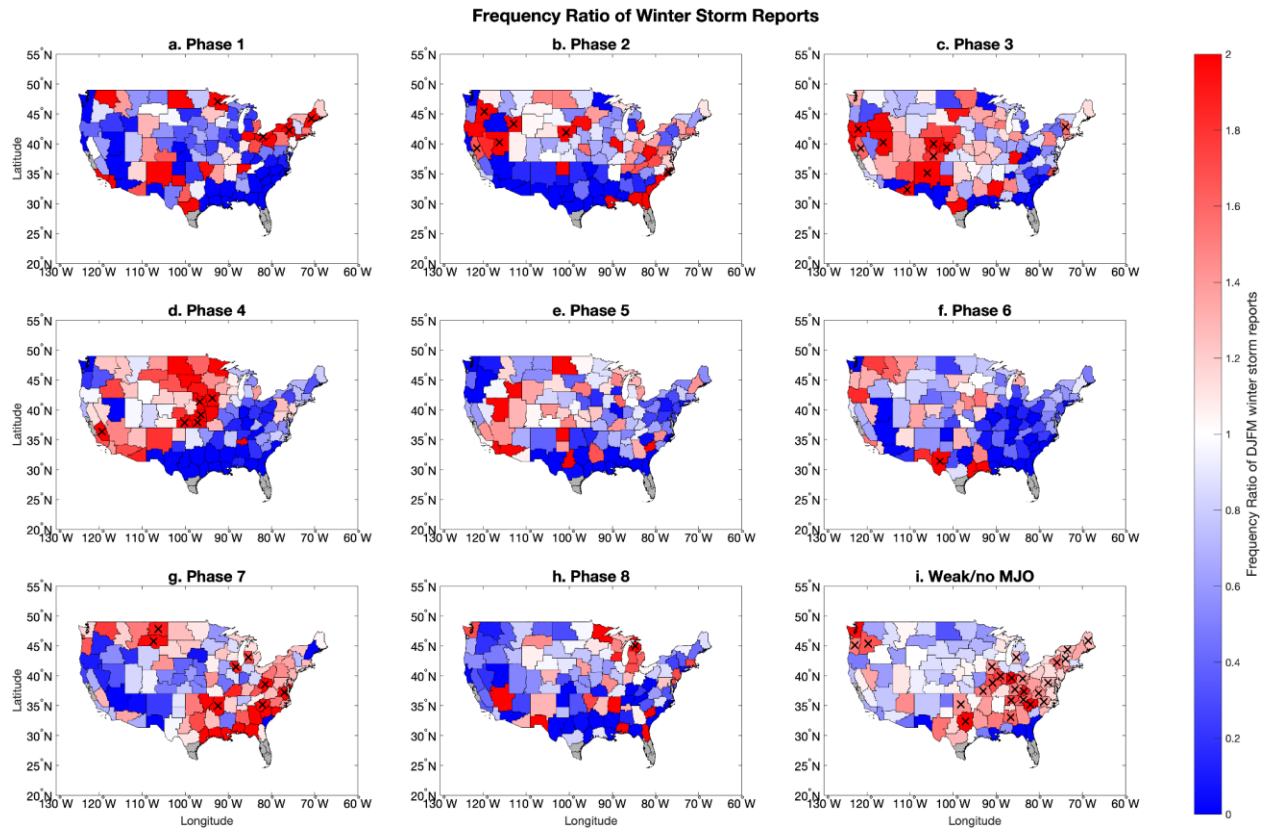


Figure 2.6: Frequency ratio for winter storm reports using RMM.

When comparing frequency ratios for winter storm reports based on RMM (Figure 2.6) and OMI (Figure 2.4) there are some broad areas of similarity with small regional sensitivities to the choice of MJO index. For phase 4 of the MJO with winter storms, both the RMM and OMI composites show high frequency ratios in the Great Plains and Mountain West, with the frequency ratios based on OMI generally having larger values in the southern tier of the country. The frequency ratios based on OMI were also higher in the Northeast. The areas of significant frequency ratios were similar for both methods, with both having significantly greater than 1 frequency ratios in the Plains during phase 4. Phase 1 also showed a significant increase in frequency ratio for winter storms in the Northeast using both OMI and RMM. However, phase 3

had more winter storms in the Mountain West when RMM was used. Phase 7 had more areas of significant winter storm frequency ratio in RMM as compared to OMI. The RMM also showed more winter storms when there were periods of weak or no MJO. Overall, there were broad similarities between the results when RMM or OMI were used. For example, phase 4 of both indices had large frequency ratios of winter weather in the Northern Plains. Phase 1 tended to have large frequency ratios in the Northeast. Since RMM can be used operationally, forecasters may take interest in the fact that similar results appear with that index as well as with OMI.

2.4. Lagged Frequency Ratio by OMI Phase

2.4.1 Definition of Regions

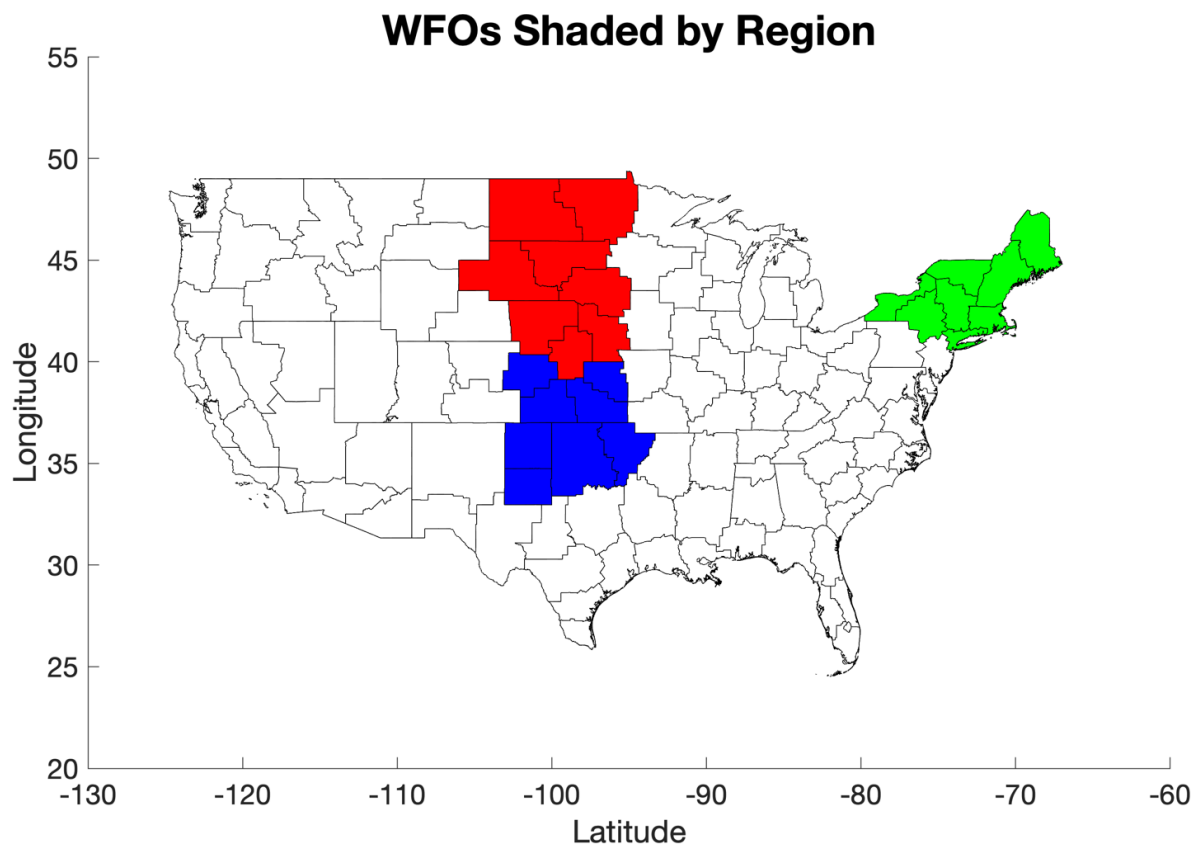


Figure 2.7: The WFOs considered to be in the Northern Great Plains (red), Southern Great Plains (blue), and Northeast (green) for the purposes of this analysis.

The Great Plains and Northeast regions were selected to provide a more in-depth analysis on how the MJO modulates the frequency of winter weather reports. These regions were selected because they all feature moderate to high frequency of winter weather events (Figure 2.1). Each of these regions have appreciable variation in winter weather event frequency. For example, in the Northern Plains, OMI phase 4 has a frequency ratio around 1.6 for winter storms, with many CWAs having double the average frequency of reports. Phase 2 in the Southern Plains and phase 1 in the Northeast have similar frequency ratios. The Northern Great Plains is colored red in Figure 2.7, and is approximately covered by the states of Nebraska, South Dakota, and North Dakota. This region has generally been considered to be a part of the Northern Plains as defined in previous work (e.g., Black 1971). It tends to feature moderately high frequencies of heavy snowfall and winter storm events, while it is just northwest of the region of most frequent ice storms. The Southern Great Plains is colored in blue, and is approximately covered by the states of Kansas and Oklahoma, along with the Texas Panhandle. It has less frequent winter weather and heavy snow events, but more frequent ice storms when compared to the Northern Plains (Figure 2.1). This region was discussed by Mullens et al. (2016), when they analyzed the synoptic conditions that led to the formation of winter weather over the Southern Great Plains. Throughout the remainder of this thesis, the terms Northern Plains and Southern Plains will be used interchangeably with Northern Great Plains and Southern Great Plains, respectively. The Northeast is colored green and is covered by New England, New York, and the northernmost parts of Pennsylvania and New Jersey. The Northeast experiences frequent heavy snowfall (Figure 2.1a), and some research has already been conducted on the effects of the MJO on

snowfall in eastern New England (Klotzbach et al. 2016), which covers approximately the eastern third of the region shaded in Figure 2.6.

2.4.2. Frequency Ratio by Region with Lag

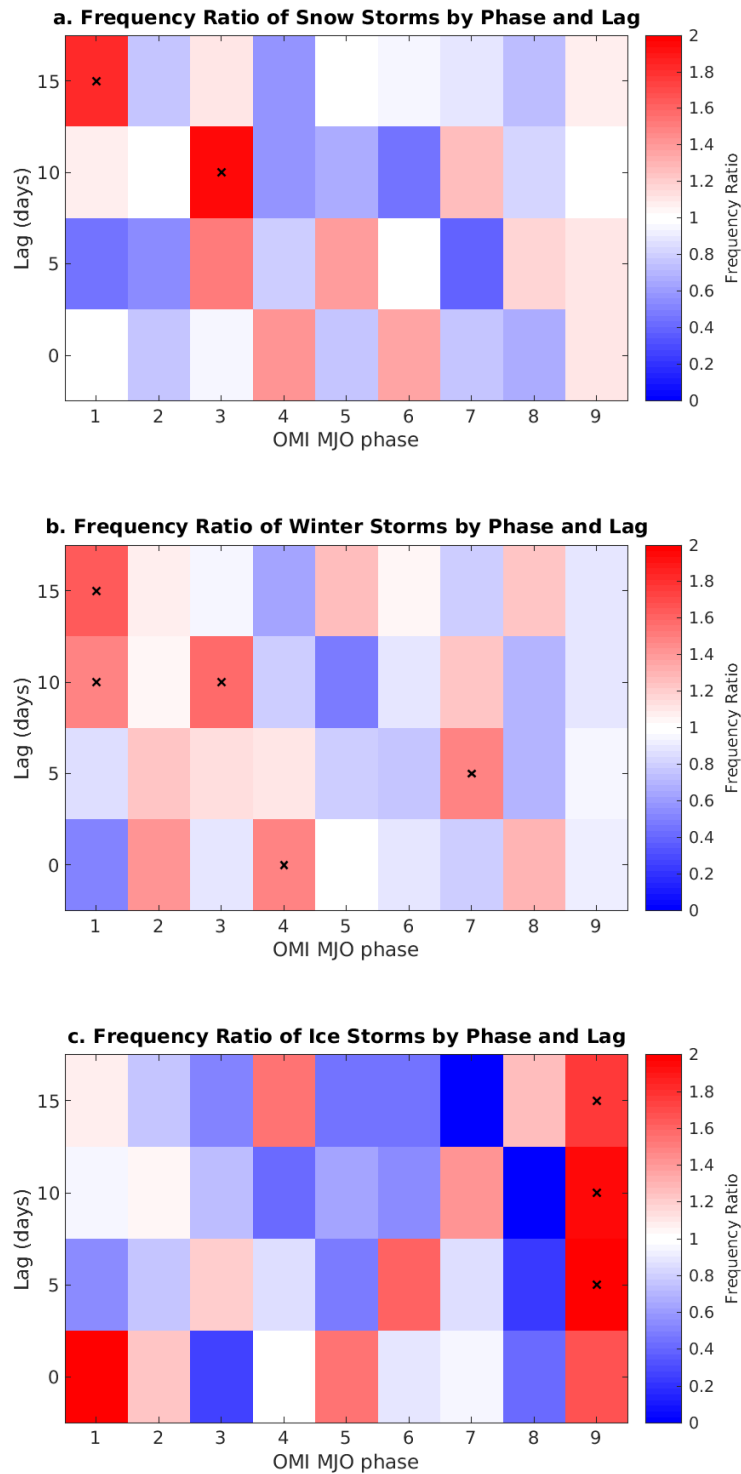


Figure 2.8: Lagged frequency ratio for winter weather reports in the Northern Plains. Phase 9 is for days with weak or no MJO. X's mark statistical significance.

The lagged frequency ratio for the Northern Plains shows the change in frequency ratio of heavy snow events at different lag times (Figure 2.8). Lag in this case is defined as the number of days after a given MJO phase occurs. Given that each MJO phase lasts approximately five days (Tseng et al. 2017), the frequency ratio for a phase with a 5-day lag should roughly correspond with a no-lag frequency ratio for the following phase. The staircase pattern visible in Figure 2.8a indicates that that is the case. So, these results indicate that some prediction skills of severe winter weather can be gained using the state of the MJO. For example, the frequency ratio at 15 days after OMI phase 1 is about 1.6. This implies that 15 days after OMI phase 1, there is a 60% increased likelihood of a heavy snowfall in the Northern Plains. This is actually a stronger relationship than during phase 4 of the MJO, where the frequency ratio is only around 1.4. The staircase pattern is, however, imperfect, as the frequency ratio at 10 days after OMI phase 2 is less than 1. Still, it can be seen that the frequency ratio with a given lag in a given phase is often similar to that of the previous phase with 5 days more of lag. The plots over regions also smooth out some of the noise. For example, phase 6 has high frequency ratios over North Dakota, but low frequency ratios over South Dakota and Nebraska (Figure 2.2). This evens out to near-normal frequency ratios overall. So, this technique works well for detecting broad trends as opposed to more localized ones.

The lagged frequency ratio for winter storms in the Northern Plains shows less pronounced variation; however, the staircase pattern is still visible (Figure 2.8b). For example, even though the largest frequency ratios were only around 1.7, that result is significant 15 days after phase 1. That matches up well with the value of around 1.5 during phase 4. It also occurs with lower frequency ratios, as there is a frequency ratio of approximately 0.9 in phase 7, and 0.8

15 days after phase 4. Frequency ratios less than 1 are also found 5 days after phase 6 and 10 days after phase 5.

For ice storms, there is not the same stairstep pattern as there is for heavy snowstorms or for winter storms (Figure 2.8c). This is likely due to the small sample size of ice storms in that region. Thus, predictability of ice storms based on MJO phase may be less than that of winter storms or heavy snow events. The only significant results occur in days after weak or no MJO at all lag times, which suggests the MJO may inhibit ice storm development on the Northern Plains.

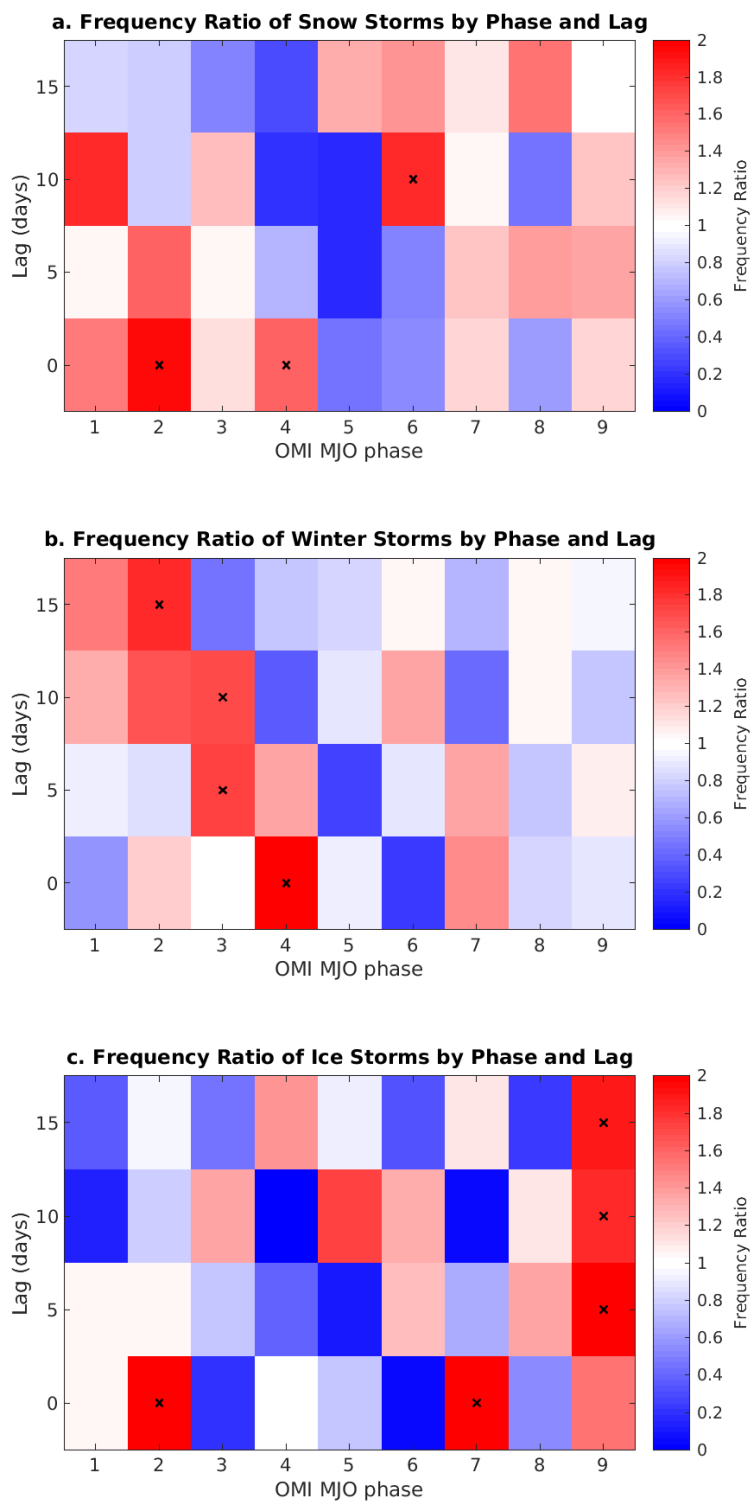


Figure 2.9: Same as Fig. 2.8, but for the Southern Great Plains.

In the Southern Great Plains (Figure 2.9), the same staircase pattern is visible, especially for winter storms. The phases with increased or decreased frequency of winter weather are similar to those of the Northern Great Plains. Winter storms are roughly twice as common as climatology in phase 4 of the OMI, but continue to be about 1.6 times as common as climatology 15 days after phase 2, with that result being statistically significant (Figure 2.9b). A similar pattern is seen with almost no winter storms in phase 6, and also almost no winter storms 15 days after phase 3. This again suggests one can predict periods of more or less risk for severe winter weather based on the phase of the MJO.

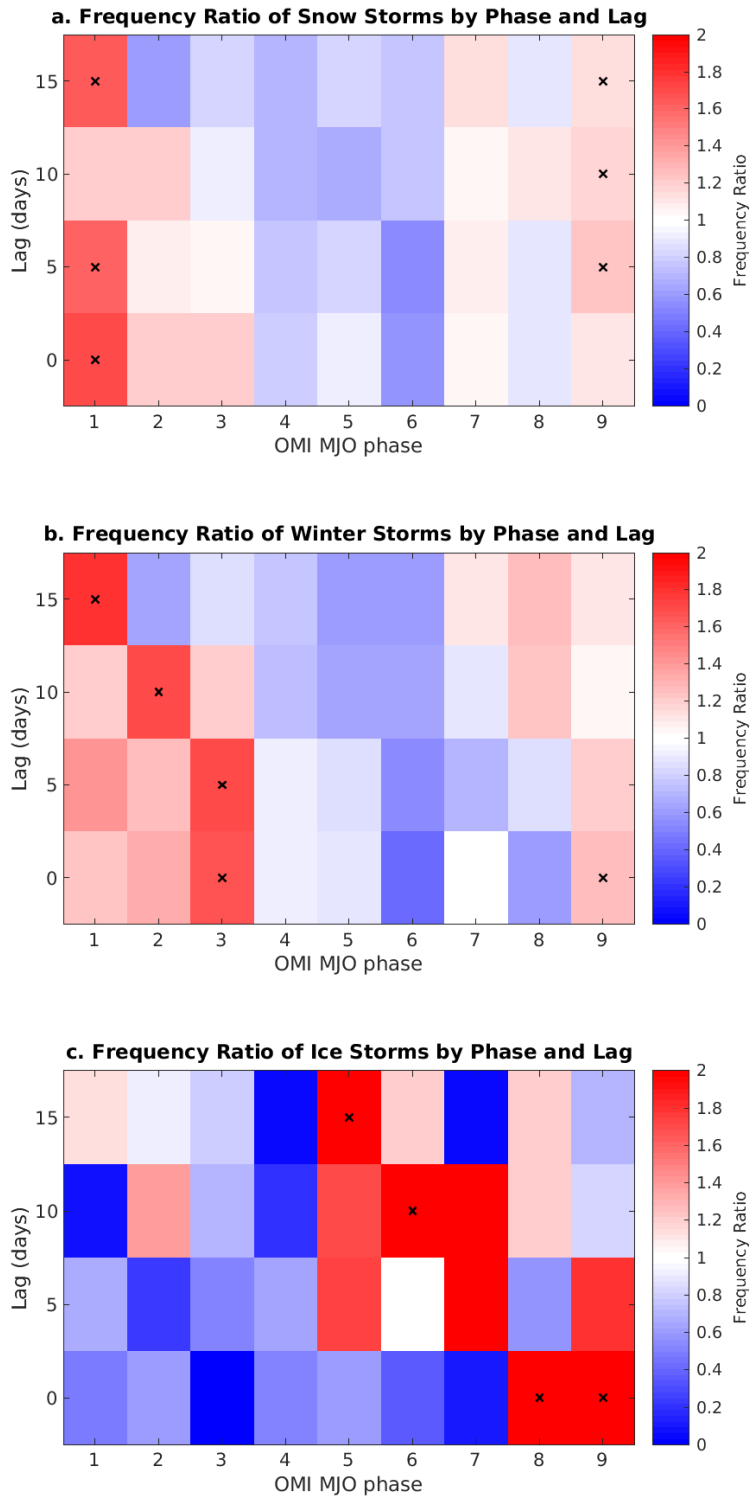


Figure 2.10: Same as Fig. 2.8, but for the Northeast.

For winter weather in the Northeast (Figure 2.10), the trends were less pronounced. Phase 1 tended to have higher frequency ratios for heavy snow and winter storms at all lag times, while phases 4-6 tended to have lower frequency ratios (Figure 2.10a, b). In addition, the frequency ratios tended to be closer to 1 for all phases and lags as compared to the Great Plains. This is the case even though both areas had WFOs with significantly greater than 1 frequency ratios. This suggests the Northeast might have more smaller scale variations that interfere with broader trends. On the other end, ice storms had more pronounced large frequency ratios than winter storms or heavy snow events, with significant frequency ratios at double the mean 15 days after phase 5 (Figure 2.10c). Previous authors (e.g., Cassou 2008, Riddle et al. 2013) have found elevated probabilities of -NAO about 10-15 days after MJO phase 7, which tends to be associated with increased frequency of winter weather in the Northeast. However, here the frequency ratios are only slightly greater than 1 and not significant. This suggests the MJO/NAO teleconnections may have limited impacts on the frequency of winter weather over the Northeast, at least in relation to either of them being compared separately.

All three regions were notable in having high frequency ratios in phases 1-3 and lower frequency ratios in phases 5-6. However, phase 4 was high on the Great Plains and low in the Northeast.

2.5. MJO Impacts on Precipitation and Snowfall Using Station Data

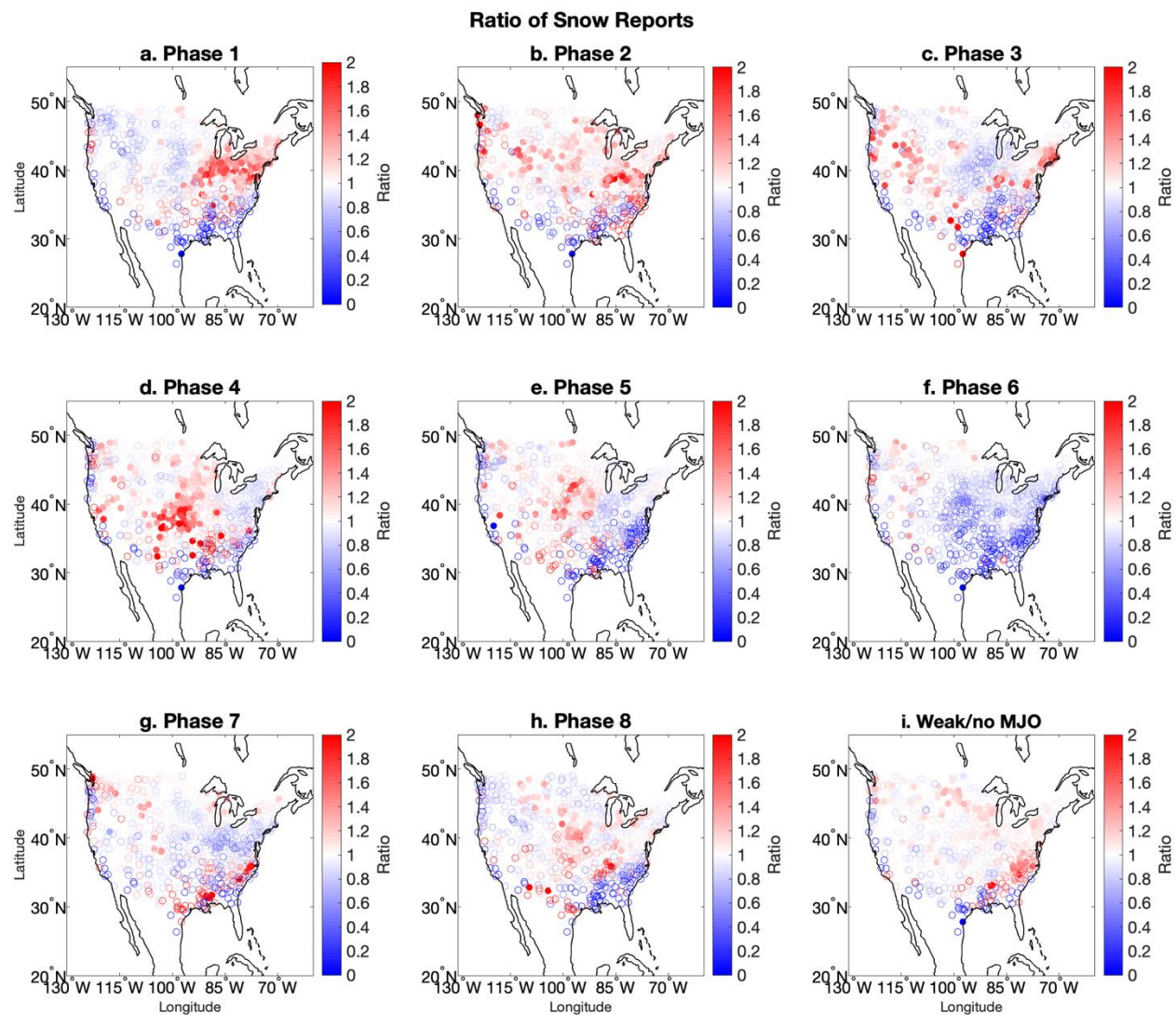


Figure 2.11: Ratio of observed snowfall to actual snowfall by OMI phase. Filled circles represent statistical significance.

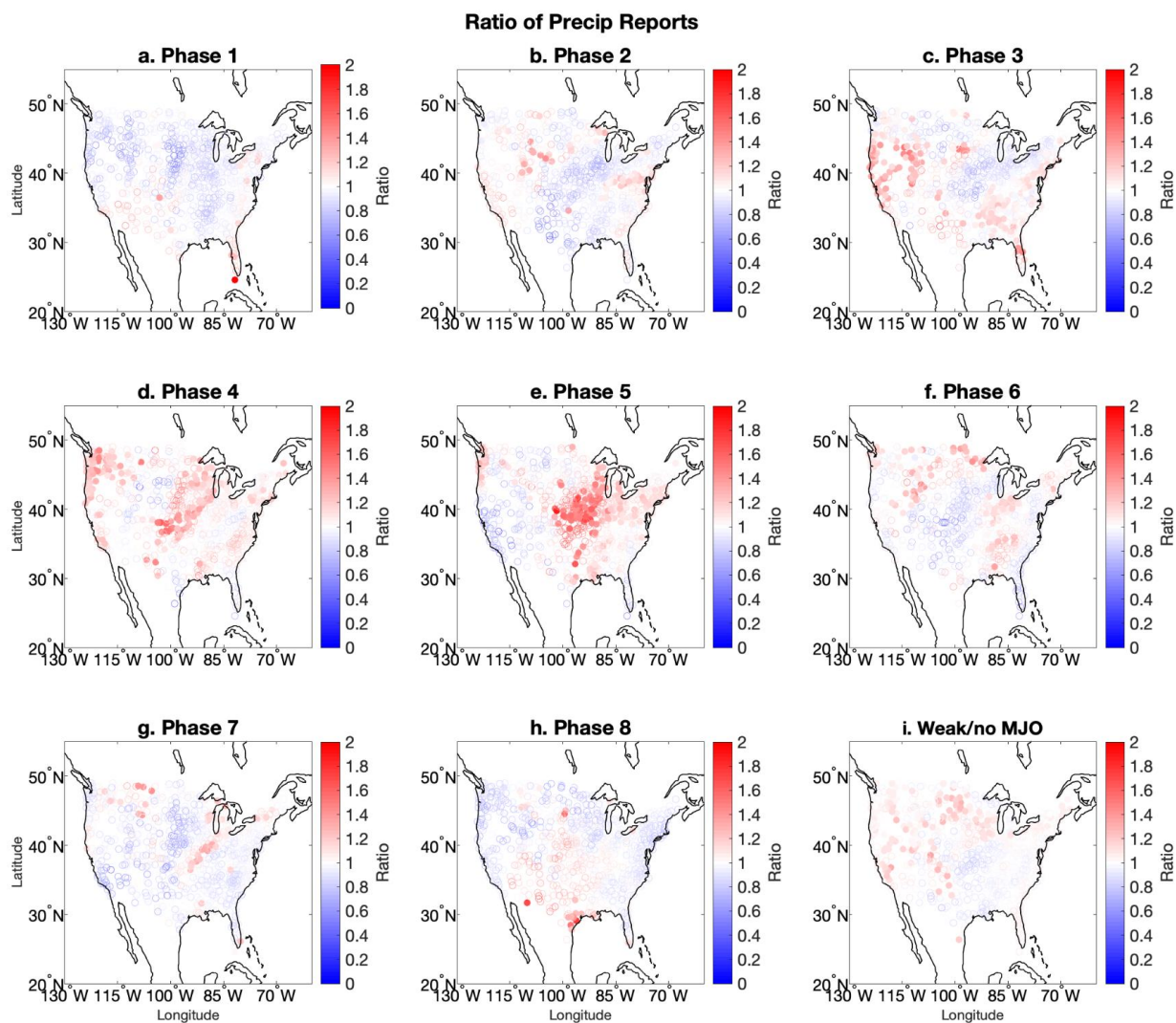


Figure 2.12: Ratio of observed precipitation to actual precipitation by OMI phase.

The ratios of observed snowfall to mean snowfall by OMI phase based on GHCN station data reports (Figure 2.11) show similar patterns to MJO impacts on NCEI heavy snow reports (Section 2.2.2). For example, OMI phase 4 has high frequency ratios of heavy snow reports in the Central and Northern Plains in the NCEI dataset and high accumulation ratios in the GHCN dataset. Phase 1 has high frequency ratios in the Northeast in the NCEI dataset and high accumulation ratios in the GHCN dataset. Most of the country has low frequency ratios and

accumulation ratios for snowfall in phases 5 and 6. These results suggest that snowfall data by MJO phase is rather consistent between the two datasets. Areas of significant ratios were often larger for snow accumulations than for snow reports. For example, phase 2 only had areas of significantly above normal frequency ratio for a few CWAs when looking at heavy snow reports, but a larger portion of the northern half of the country had significantly increased snow accumulation (Figure 2.11b). Phase 3 similarly had large areas of significant frequency ratios in both the Northeast and Northwest United States.

In many areas of the country (e.g., the Great Plains and Midwest during phase 4), precipitation (Figure 2.12d) and snowfall (Figure 2.11d) ratios of 1.2 to 1.3 were significant in the GHCN dataset. However, heavy snow frequency ratios were often closer to 2 in the NCEI dataset (Figure 2.3d). If heavy snow frequency ratio magnitudes in the NCEI dataset are much larger than snow accumulation ratios in the GHCN dataset, that suggests snowfall in that phase is dominated by more frequent major events. For example, if the NCEI dataset has double the number of storms with at least 4" (10 cm) of snow, for a frequency ratio of 2, but the total snow accumulation in a given phase was only 20% greater than normal, the proportional snow accumulation from smaller events will be fewer. If the reverse is true, that suggests snowfall is dominated by minor events. Precipitation and snowfall can be analyzed together to determine how much of the anomalies in snow accumulation ratios were caused by changes in precipitation. There are certain phases and regions, such as phase 2 in the Mid-Atlantic and Mountain West, and phase 4 in the Great Plains, where there is both above normal snowfall and precipitation according to GHCN data. So increased precipitation can be associated with increased snow accumulations.

Precipitation could also be compared to winter storm and ice storm frequency ratios to see if precipitation accumulation had an impact on those values. This is useful because GHCN data are not available for freezing rain or sleet accumulation. The central U.S. experiences increased precipitation (Figure 2.12d, e) and increased frequency of winter storms in OMI phases 4 and 5 (Figure 2.4d, e). Phase 3 in the western U.S. features a similar pattern. This suggests that the impact of the MJO on precipitation can lead to increased frequency of storms containing some amount of sleet or freezing rain. In contrast, no significant increase in precipitation appears over the Northeast during phases 1-3 when snowfall and winter storm reports are enhanced. This suggests that, over the Northeast during phases 1-3, if a precipitating storm formed over the region, its precipitation would preferentially occur in the form of ice and snow, rather than rain, while the overall frequency of storm formation would not change. The reasons for differences in how the MJO influences regional winter weather will be further investigated in the next chapter. Given that freezing rain is not recorded separately from precipitation, the precipitation accumulation ratios can be compared to the temperature anomalies shown in the next chapter to determine if the precipitation was more likely to be freezing. GHCN data were from 1979-2020 as compared to storm data from 1996-2018. The fact that the GHCN snow maps were similar to the storm report maps in spite of the differing time periods suggests that the results are robust when compared to changes in the period of record as well.

3. Physical Mechanisms Behind MJO Impacts on Winter Weather

The objective of this section is to examine which atmospheric conditions are associated with the MJO and act as a potential mechanism for the MJO to influence winter weather over the United States. Thus, it will discuss not only how the MJO influences intraseasonal atmospheric conditions but also what synoptic conditions are associated with the occurrence of winter weather events, and how they relate.

3.1. Data and Methods

Atmospheric conditions associated with the MJO and winter weather events were analyzed using data at 6-hourly intervals from the ECMWF Reanalysis v5 (ERA5) in the months DJFM from 1996-2018. ERA5 was chosen due to its reliability and accuracy (Hersbach 2020). ERA5 was established as a replacement for ERA-Interim, and it features a 31-km grid resolution, 137 vertical levels to 1 Pa, 4D-Var data assimilation, and advanced ocean, soil, and climate modeling (Hersbach 2020).

Many atmospheric variables are used in synoptic-scale weather forecasting to predict the development of a cyclone resulting in winter weather. The goal of this chapter is thus to determine if a given phase of the MJO causes changes in those variables that would be associated with storms producing severe winter weather. Some of these variables include temperature, wind, geopotential height, and specific humidity, which are analyzed here. We hypothesize that the midlatitude Rossby wave train that is initiated by the MJO develops an anomalous trough over different regions of the CONUS. The trough can then generate anomalously cold and moist regions, supporting the development of severe winter weather.

To test this hypothesis, surface temperature composites and anomalies were also analyzed to best determine the likely precipitation type and likelihood of snow accumulation. Surface temperatures must be below freezing for freezing rain to occur, and snow is more likely and accumulates faster when surface temperatures are below freezing. Temperature was analyzed at 850 hPa as well, which is compared with the surface temperature to detect inversions. Wind speed and direction are important for determining regions of anomalous cyclonic or anticyclonic circulation. Wind at 850 hPa could be compared to temperature at that level to find areas of temperature advection. Warm advection is often associated with rising motion in cyclonic storm systems. Geopotential height at 500 hPa is another variable that was analyzed. It is used to detect areas of ridging and troughing. Geopotential height was analyzed with wind at the 250-hPa level. This provides a sense of wind at the tropopause near where jet streaks form and shows how jet dynamics can relate to areas of ridging and troughing in the lower atmosphere. Specific humidity at 700 hPa was analyzed along with winds at that level to identify the regions of anomalous moisture and how it was advected. Anomalous moisture can lead to the development of clouds and precipitation. Surface pressure was analyzed to determine the location of surface lows.

To analyze these variables, composites were made of the average values of the variables by OMI phase. To create composites of atmospheric variables, the values on each day in a given phase were summed and then divided by the number of days in that phase. Then a climatology was constructed by finding the mean values from the years 1996-2018 for each day from December 1 to March 31 regardless of OMI phase. Once the composites and climatologies were created, anomalies were calculated by subtracting the composite values from the climatology. These variables were looked at in two different geographical ranges: one covering the United

States and surrounding areas from 130°W to 60°W and 20°N to 55°N, and one covering the parts of the Northern Hemisphere from 135°E to 0°. The Northern Hemisphere region includes the area from the equatorial tropics where the MJO originates, North America, and also the North Atlantic, where Atlantic blocking takes place.

Additionally, composites were made of the previously mentioned variables for days that a winter weather event occurred in the Storm Event Database (referred to as storm days). This was done to compare the atmospheric conditions when winter storms occurred to those conditions in a given phase of the OMI. If there was overlap between the two results, that would suggest that the conditions in a given phase of the OMI are supportive of winter weather occurrence. The amount of overlap was computed using a spatial correlation between the two composites. A positive correlation close to one would suggest that the patterns when a given storm type occurred were similar to those in a given phase of the MJO. For storm day composites, winter weather events were only chosen if they occurred within one of eight county warning areas (CWAs) located on either the Northern or Southern Great Plains or the Northeast (Figure 2.7). These regions were selected to coincide with those from Section 2.4 and also determine regional differences in how the MJO impacts winter weather.

Significance tests were also conducted for all of the variables except wind. This is because wind was typically analyzed in a manner secondary to another variable such as 850-hPa temperature, 500-hPa height, or 700-hPa specific humidity. Significance tests were conducted using a Monte Carlo method over the 1996-2018 time period, with a two-tailed 95% significance threshold. A total of 1,000 samples were used. This was done over the entire DJFM sample period for events by storm day and OMI phase.

3.2. Results

3.2.1. Surface Temperature Anomalies

While snowfall can occasionally accumulate with temperatures above freezing, snow accumulates more readily when air temperatures are below freezing. Furthermore, surface temperatures must be below freezing for freezing rain to occur. Thus, surface temperature anomalies are important to determine if precipitation in a given OMI phase is more likely to fall as snow or freezing rain as opposed to rain. There are statistically significant variations in surface temperature anomalies by MJO phase across much of the United States (e.g., Zhou et al. 2012, Matsueda and Takaya 2015, Zhou et al. 2011) (Figure 3.1). Phase 1 has cooler than normal values over much of the Northeast U.S., where there were also high frequency ratios for heavy snow and winter storms (Figures 2.3a, 2.4a). This implies that the increased frequency of winter weather events during phase 1 over the Northeast could be due to the effect of below normal temperatures that is associated with the MJO. Phase 5 is warm in the Southeast and lacks areas of significant high frequency ratios for any storm type (Figure 2.3e). Phase 6 is warm across much of the eastern and central part of the country, while phase 7 is cold in the far north into Canada (Figure 3.1), with neither phase having more than a few CWAs with significant high frequency ratios (Figures 2.3 and 2.4 f, g). Phase 8 is cold in Maine and the Canadian Maritimes, but the areas of high frequency ratios for winter weather were in the Central U.S. (Figure 2.4h), and there were no significant areas of high frequency ratios for heavy snow (Figure 2.3h). Phase 2 featured cool temperature anomalies over much of the country and phase 4 had warm anomalies, but neither set of anomalies were significant (Figure 3.1). Similarly, phase 3 had near-normal temperatures across most of the country.

Given teleconnections between the MJO and NAO have been found (e.g., Cassou 2008, Lin et al. 2009), it is worth comparing the temperature anomalies associated with the MJO to those associated with the NAO. The surface temperature anomalies in phase 5 were most similar to those in the positive phase of the NAO, while the anomalies in phase 8 were most similar to a negative NAO (Greatbatch 2000). However, while the negative phase of the NAO is associated with snowfall in the Northeast U.S., (Hartley and Keables 1998), our results showed near-normal snowfall in phase 8 and more snow in phase 1 in that region. Direct analysis of the NAO and MJO together in the region may be necessary to provide further insight on this discrepancy.

These results had some similarities to the temperature composites of Zhou et al. (2012) (Figure 1.2) but also some differences. Our results and those of Zhou et al. (2012) both captured cold anomalies in the northern U.S. in phases 1 and 8, and warm anomalies in the eastern part of the country in phases 5 and 6. However, in phase 1, Zhou et al. (2012) found the core of the cold temperature anomalies to be centered in the Upper Midwest, while we found the greatest cold anomalies to be in the Northeast. Phases 2 and 4 tended to have weaker surface temperature anomalies in our results as compared to those found by Zhou et al. (2012). One potential cause of the differences is the use of a different index to categorize the phase of the MJO. Our results use OMI while Zhou et al. (2012) used RMM. Also, our composites were for the months of December through March from 1996-2018, while Zhou et al. (2012) only used December through February from 1979-2008.

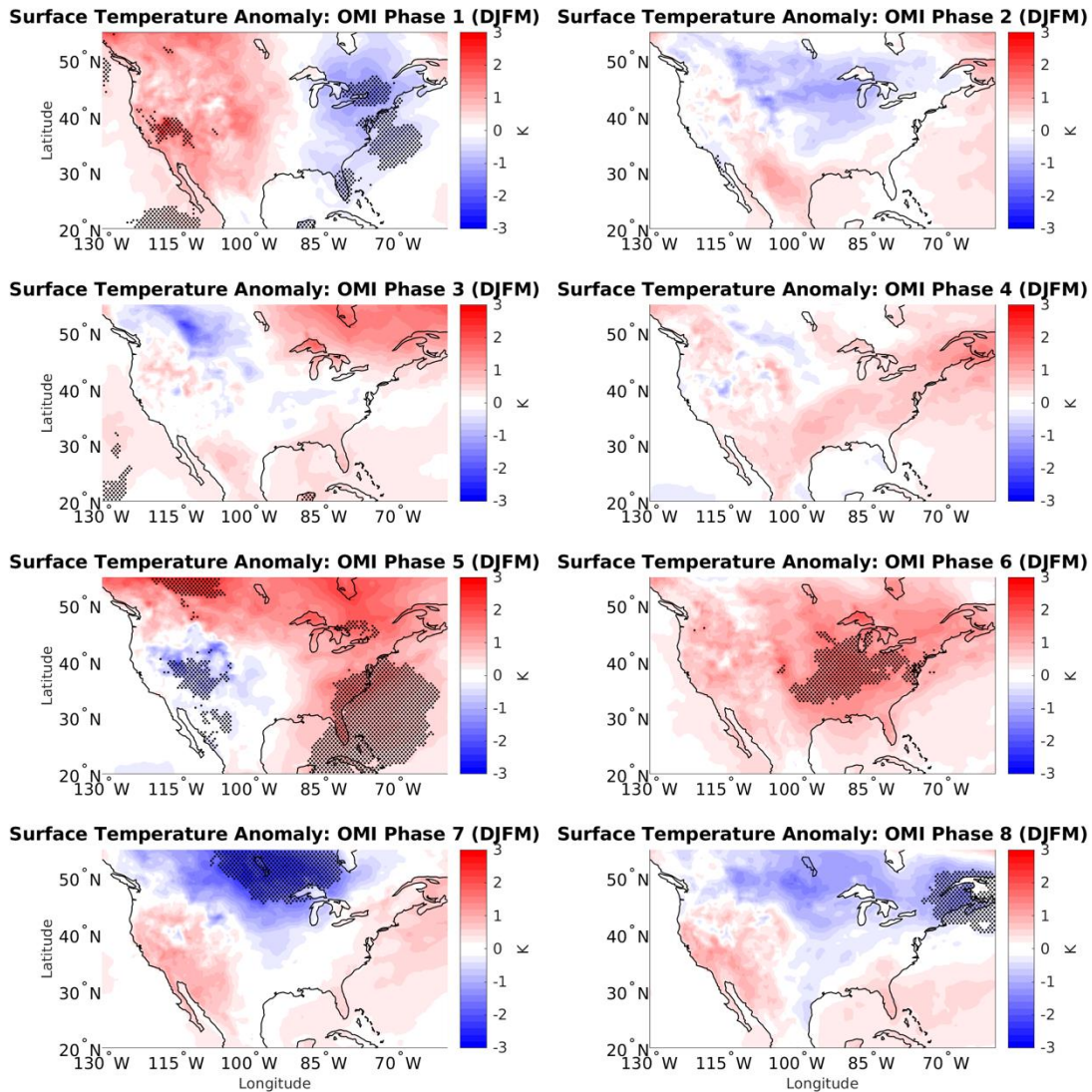


Figure 3.1: Surface temperature anomaly by OMI phase. Stippling in this and other figures in this chapter represent statistical significance at the 95% level.

To determine to what extent the influence of the MJO on surface temperature affects the frequency of winter weather events, we will analyze how the temperature anomalies in a given phase of the OMI compare to the temperature anomalies on days with given types of winter weather events in the regions of the country shown in Figure 2.7. If a given OMI phase has a high frequency of winter weather events and a similar temperature pattern to days with winter

weather events, that suggests that the MJO's influence on temperature may be part of the reason for the high frequency of winter weather events in that phase. The spatial correlation of the temperature anomalies by OMI phase to those by storm days will be computed to assess their similarity.

On days with winter weather events in the Northern Plains (Figure 3.2), most of the eastern and central U.S. have significant warm anomalies of around 2 K for heavy snow and winter storms, and 4 K for ice storms. Meanwhile, the northern Mountain West and far Northern Plains tend to be cooler than normal. These increased temperature gradients over the Northern Plains region could be indicative of frontal systems. Ice storms are the only storm type with no significant cool anomalies in or near the United States. However, only a weak increase in temperature gradient is observed over the Northern Plains during phase 4 of the OMI (Figure 3.1) when winter weather reports are higher there (Figure 2.3d, 2.4d). This result suggests the modulation of surface temperature anomalies is not the main reason why phase 4 of the OMI tends to support severe winter weather over the Northern Plains. The spatial correlations between OMI phase and heavy snow and winter storm days were positive in phases 2 through 4, as well as phase 6 (Table 3.1). None of the phases with negative correlation had above normal frequency of heavy snow days. This suggests that some of the temperature patterns associated with heavy snow in the Northern Plains may be due to associations between the MJO and temperature, but there are other factors as well.

The surface temperature associated with winter weather reports over the Southern Plains (Figure 3.3) has a similar pattern to the Northern Plains; however, the areas of cold and warm anomalies are shifted to the south. The magnitude of the warmest temperature anomalies is weaker than in the Northern Plains. Furthermore, for ice storm days in the Southern Plains, there

is an area of significant colder anomalies to the northwest. These patterns are largely similar to the anomalies found in OMI phase 2, except that the OMI anomalies are not statistically significant. There are high (0.51 to 0.73) spatial correlations between temperature anomalies during days with winter weather and OMI phase 2 (Table 3.2), which suggests that the relationship between temperature and the MJO in that phase is associated with its effects on winter weather event frequency.

In the Northeast (Figure 3.4), the pattern is slightly different. In days with winter weather in that region, the areas of greatest warm anomalies are located due south or southwest of the region. This is most similar to OMI phase 2, which had frequency ratios near to above normal (Figures 2.3b, 2.4b). This is in contrast to the areas of greatest warm anomalies being located to the southeast when there is winter weather in the Great Plains. The pattern in the Northeast could be different because the Atlantic Ocean is to the southeast of the region, where the standard deviation in temperature is lower. Ice storm days in the Northeast have the greatest warm anomalies, with maximum values close to 7 K in the Ohio Valley. This could be due to low pressure areas passing to the north of the valley in such situations, with winds bringing warm air from the south. Here the strongest correlations between temperature anomalies by OMI phase and storm days are in phases 2 and 7 (Table 3.3), both of which had frequency ratios near 1 (Figure 2.10). This means that in the Northeast, spatial correlations of temperature do not suggest a relationship between the MJO and winter weather through surface temperature.

A few regions have statistically significant temperature anomalies despite small magnitudes of the anomalies. This is because the temperature climatology is from 1981-2010, while the dataset of storm days is from 1996-2018. Due to climate change, temperatures across the United States have warmed slightly, so the mean anomaly will be slightly greater than zero.

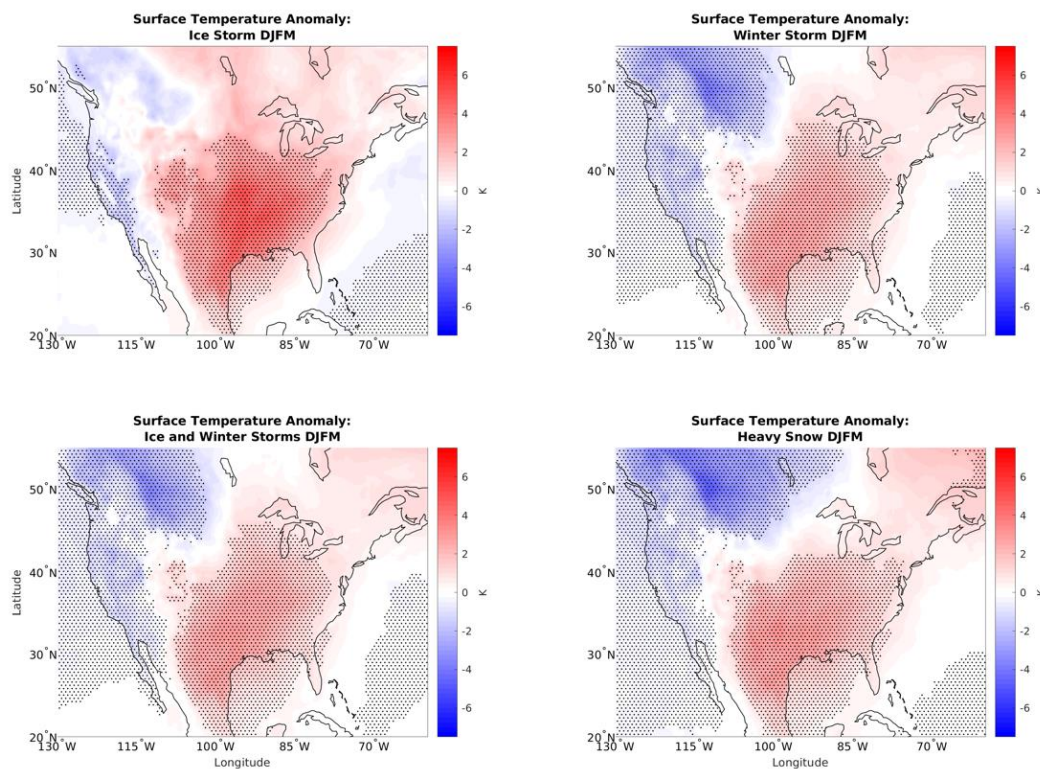


Figure 3.2: Surface temperature anomaly associated with different types of winter weather events on the Northern Great Plains.

Table 3.1: Correlation between surface temperature anomalies on days with given storm type in the Northern Plains and OMI phase

OMI Phase	1	2	3	4	5	6	7	8
Heavy snow	-0.64	0.21	0.41	0.25	-0.30	0.18	-0.08	-0.08
Winter storm	-0.59	0.10	0.38	0.29	-0.19	0.32	-0.22	-0.22
Ice storm	-0.21	-0.25	-0.04	0.30	-0.07	0.58	-0.21	-0.38

Note: In this and all following tables in this chapter, OMI phases that had statistically significant high frequency ratios for a given winter weather type are shown in bold.

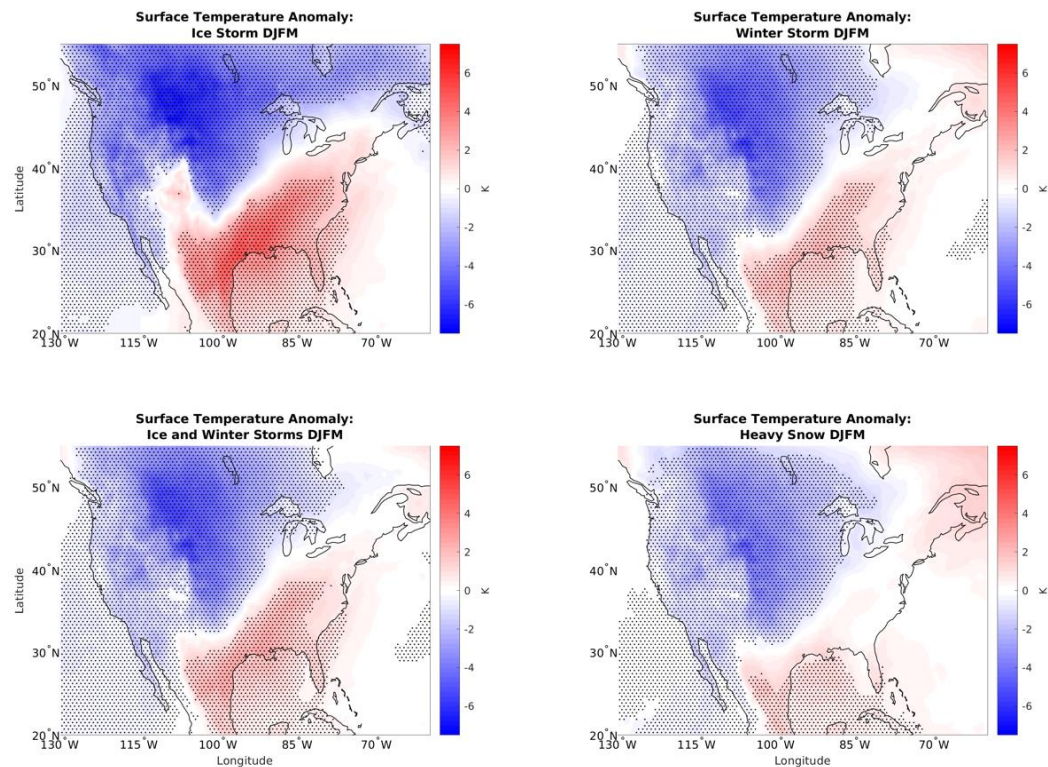


Figure 3.3: Same as Fig. 3.2, but for the Southern Great Plains.

Table 3.2: Correlation between surface temperature anomalies on days with given storm type in the Southern Plains and OMI phase

OMI Phase	1	2	3	4	5	6	7	8
Heavy snow	-0.62	0.73	0.38	0.08	0.01	-0.42	0.30	0.17
Winter storm	-0.70	0.61	0.44	0.09	-0.08	-0.28	0.35	0.19
Ice storm	-0.61	0.51	0.12	-0.02	-0.37	-0.25	0.49	0.35

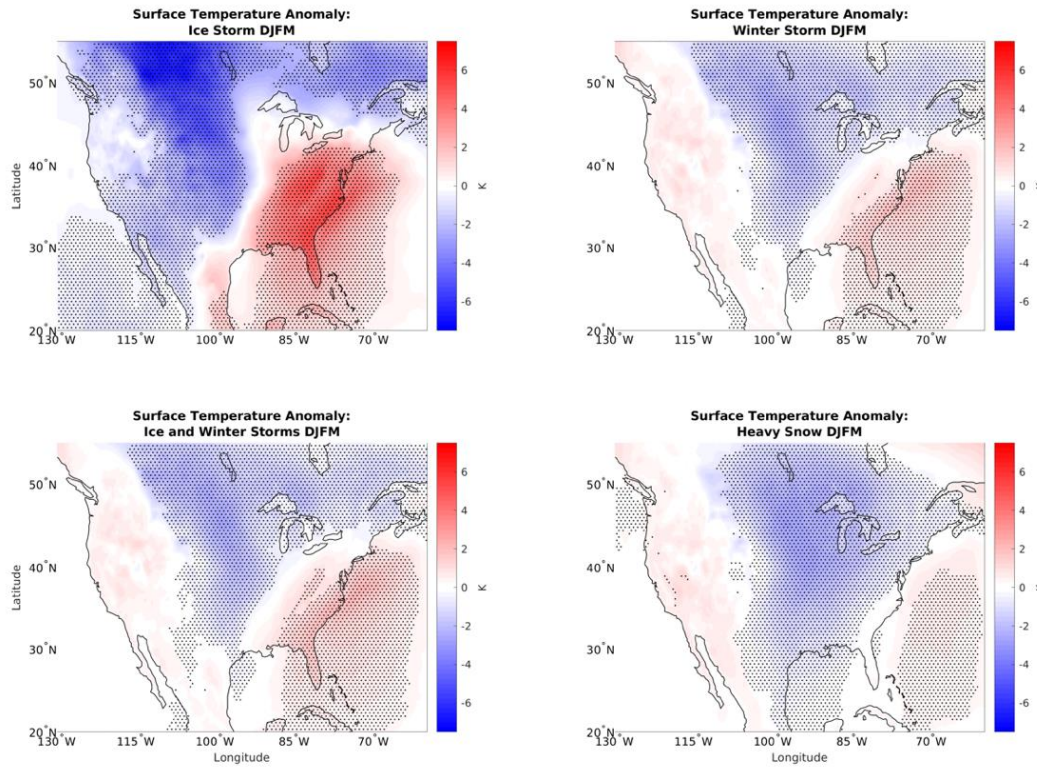


Figure 3.4: Same as Fig. 3.2, but for the Northeast.

Table 3.3: Correlation between surface temperature anomalies on days with given storm type in the Northeast and OMI phase

OMI Phase	1	2	3	4	5	6	7	8
Heavy snow	-0.03	0.63	0.06	-0.27	-0.36	-0.80	0.68	0.66
Winter storm	-0.35	0.50	0.01	-0.22	-0.37	-0.56	0.69	0.68
Ice storm	-0.71	0.30	0.17	-0.02	-0.19	-0.08	0.43	0.36

3.2.2. 850 hPa Temperature and Wind Anomalies

The next variable analyzed is 850 hPa temperature. The freezing line at 850 hPa is often a reasonably good determinant of the precipitation type at the surface, with below freezing 850 hPa temperatures typically being necessary for snow. Furthermore, if 850 hPa temperature anomalies are greater than those at the surface, that would suggest inversions are more likely, and thus freezing rain and sleet would be more likely as precipitation types. Wind at 850 hPa is analyzed in addition to temperature to identify anomalous temperature advection. Warm air advection is often associated with isentropic ascent, where the air cools as it ascends over a colder air mass. Isentropic ascent can lead to condensation and precipitation development in extratropical cyclones.

At the 850 hPa level, the temperature anomalies are similar but not identical to those at the surface. For example, the below-normal temperature anomalies in the Northeast during OMI phase 1 are statistically significant at the surface but not at 850 hPa. Phase 7 has a larger area of cold anomalies at 850 hPa when compared to the surface. Phase 4 has slightly higher temperature anomalies at 850 hPa compared to the surface and also a very high frequency of winter storms in the Northern Plains, which have freezing rain or sleet.

The wind anomalies are often parallel to the isotherm anomalies, suggesting that the anomalous flow is approximately geostrophic (Figure 3.5). However, there are some exceptions. For example, phase 7 features anomalous cold air advection near the Gulf and Atlantic coasts, and phase 8 features anomalous cold advection over the Upper South. During phase 6, there is anomalous warm air advection from the Central U.S. into Canada. Phases 2 and 4, which have large winter weather frequency ratios over the Great Plains, tend to feature weak winds over that area. Phase 1, which has a large frequency ratio of storms over the Northeast features

significantly lower heights toward the south, with anomalous cyclonic circulation over the Northeast itself.

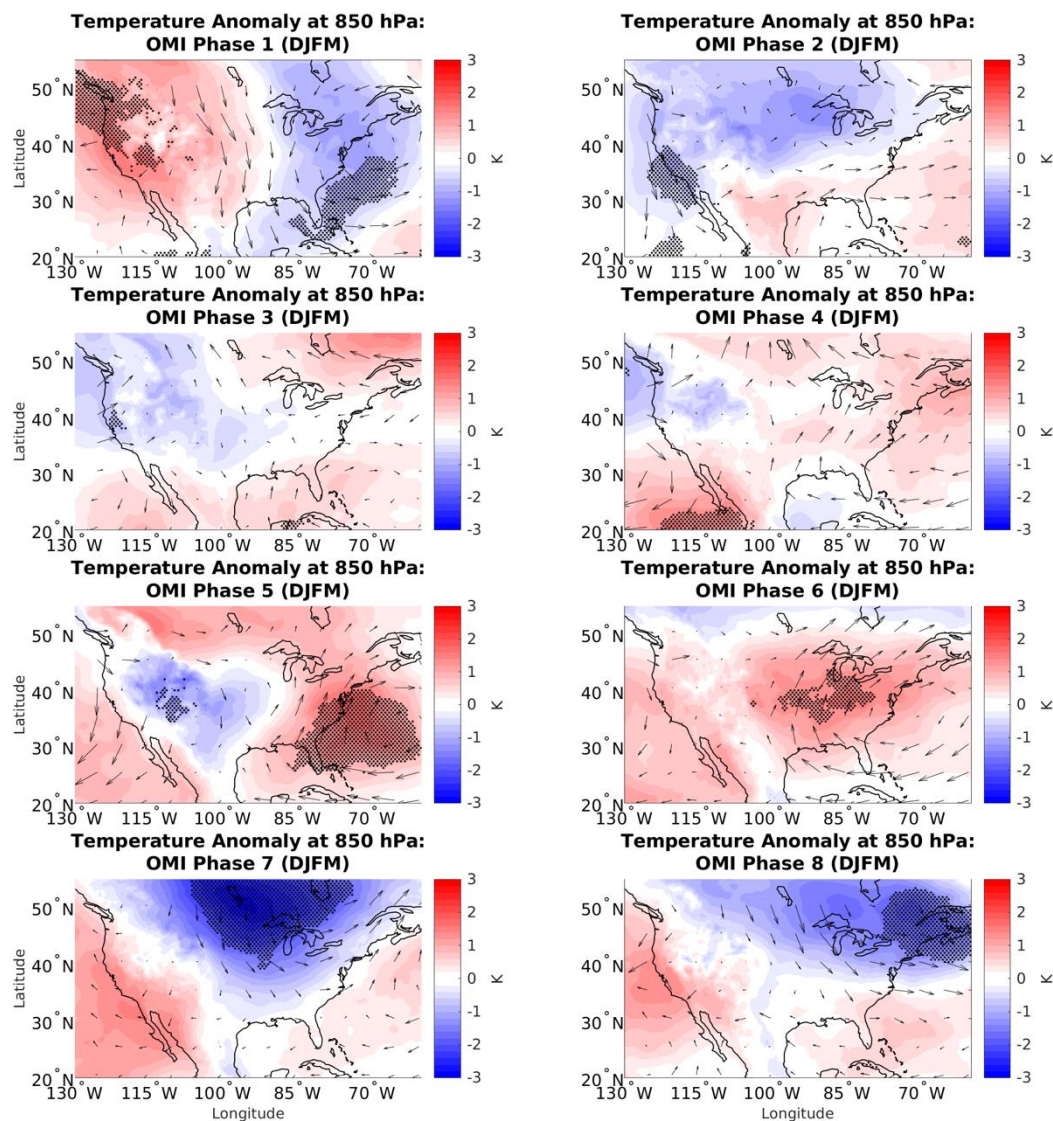


Figure 3.5: 850 hPa temperature (shading) and wind (vector) anomalies by OMI phase. For this and following plots, stippling represents areas of statistical significance for the shaded variable.

Temperature and wind anomalies at 850 hPa on days with winter weather can be compared to days in a given OMI phase in the same way that this was done for surface temperatures. Storm days in the Northern Great Plains have a large amount of anomalous warm

air advection (Figure 3.6), especially for winter storm and heavy snow events. Ice storms have the warmest 850 hPa temperature anomalies, of 3-5 K. For precipitation to be freezing rain, there needs to be a layer of the atmosphere above freezing, so these warm anomalies are in agreement with storm thermodynamics. For winter weather days in the Southern Great Plains, the temperature pattern is shifted to the south (Figure 3.7). Again, there is a large amount of anomalous warm air advection over the region of interest. The magnitudes of the cold anomalies are greater and closer to the region of interest in the Southern Great Plains case. For the Northeast, the magnitude of the warm anomalies is greater than the other regions, at 6-7 K (Figure 3.8). For all of the regions, winter storm days tend to have weak warm anomalies at 850 hPa as well. This is because winter storms have some amount of sleet or freezing rain, so they still need a warm layer over 0°C. For heavy snow days, there tend to be slight cold anomalies in the Southern Plains, where average temperatures tend to be warmer. However, temperature anomalies are closer to zero in the Northern Plains and Northeast. Similar to the surface temperature cases, there is a strong temperature gradient in each situation.

The 850 hPa temperature and wind anomalies during days with winter weather in the Northeast tend to most resemble OMI phases 2, 3, and 7 (Table 3.6) when the number of winter weather reports is near or above normal. In the Southern Plains the results most resemble OMI phase 2, with correlation values above 0.7 for all storm types (Table 3.5). In the Northern Plains the results most resemble OMI phases 2, 3, 4 and 6 (Table 3.4). These are all phases with near to above normal frequency of winter weather events in their respective regions. So, it seems that temperature and wind at 850 hPa play a role in winter weather development in all three regions. But since the OMI phase with the strongest spatial correlation does not correspond to the phase with the highest frequency of winter weather, other factors must also play a role. In the Northern

Plains, the changes in the frequency of winter weather are partially caused by increased warm advection in much of the region, leading to increased moisture, and sleet or freezing rain being more likely as precipitation types. In the Southern Plains and Northeast, the advection patterns are less pronounced, but the temperature patterns are still present. The increased temperature gradient could lead to baroclinicity and storm development.

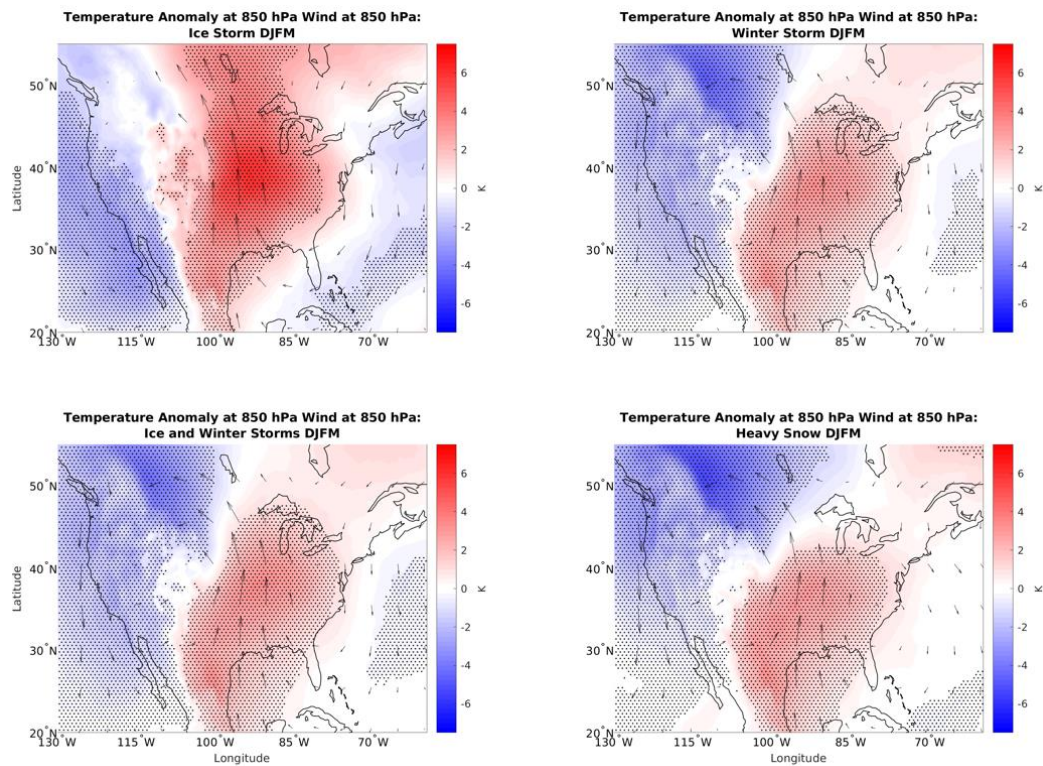


Figure 3.6: 850 hPa temperature and wind anomalies associated with different types of winter weather events in the Northern Great Plains.

Table 3.4: Correlation between 850 hPa temperature anomalies on days with given storm type in the Northern Plains and OMI phase

OMI Phase	1	2	3	4	5	6	7	8
Heavy snow	-0.55	0.62	0.58	0.25	-0.15	0.44	0.09	-0.08
Winter storm	-0.62	0.48	0.54	0.24	-0.06	0.47	-0.19	-0.27
Ice storm	-0.24	-0.16	0.04	0.13	-0.13	0.36	-0.72	-0.52

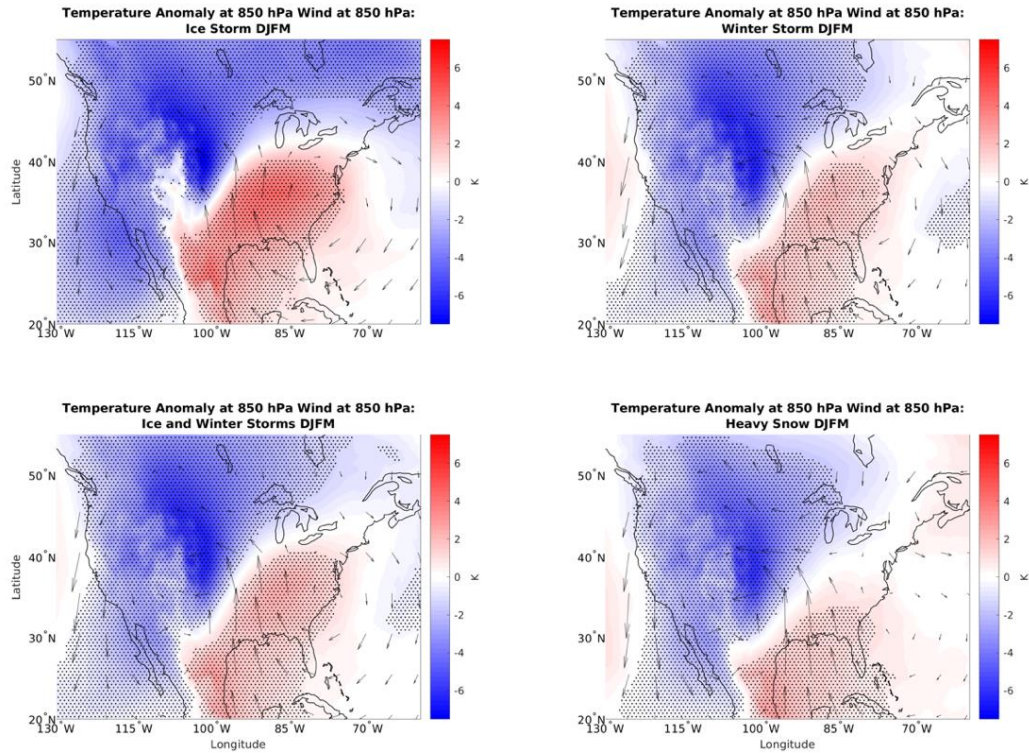


Figure 3.7: Same as Fig. 3.6 but for the Southern Great Plains.

Table 3.5: Correlation between 850 hPa temperature anomalies on days with given storm type in the Southern Plains and OMI phase

OMI Phase	1	2	3	4	5	6	7	8
Heavy snow	-0.50	0.73	0.49	0.04	0.33	-0.13	0.25	0.13
Winter storm	-0.49	0.72	0.44	0.02	0.24	0.05	0.28	0.16
Ice storm	-0.45	0.71	0.23	-0.04	0.05	0.20	0.22	0.20

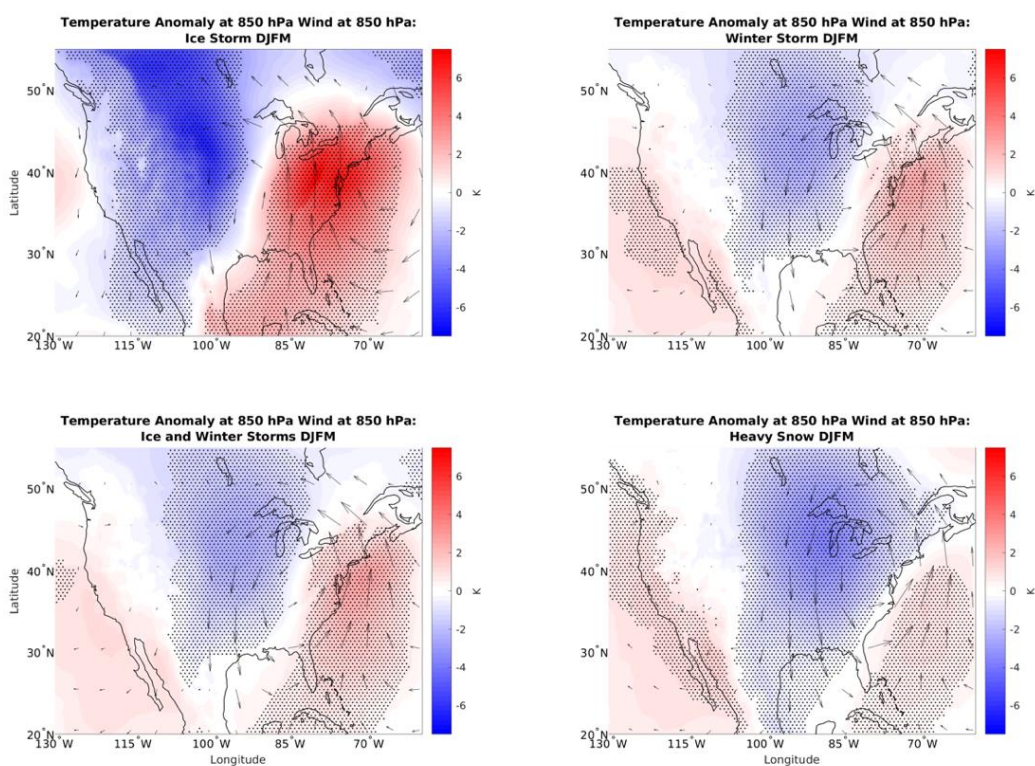


Figure 3.8: Same as Fig. 3.6 but for the Northeast.

Table 3.6: Correlation between 850 hPa temperature anomalies on days with given storm type in the Northeast and OMI phase

OMI Phase	1	2	3	4	5	6	7	8
Heavy snow	0.28	0.41	0.04	-0.11	0.03	-0.46	0.81	0.65
Winter storm	-0.17	0.56	0.22	0.06	0.31	-0.12	0.75	0.50
Ice storm	-0.70	0.56	0.37	0.08	0.41	0.33	0.23	0.06

3.2.3. Geopotential Height and Wind Anomalies

Geopotential height anomalies are important for determining areas of ridging and troughing, which can affect the wind flow and create areas that are favorable or unfavorable for cyclogenesis. Geopotential height anomalies at 500 hPa are significant in many areas based on OMI phase (Figure 3.9). Phase 1, which has increased winter weather in the Northeast, has a positively tilted trough in the east and ridge in the west. Phase 2, which has increased winter weather in the Southern Great Plains, has a trough just to the west. Phase 3 features a trough in the Northwest U.S. and large frequency ratios of winter weather reports for that region and just to the south. Phase 4 does not feature significant ridging or troughing anywhere in the country yet has high frequency ratios in the Northern Plains. Phase 6 has significant ridging in the eastern half of the country and few major winter weather events there. Areas with troughing and anomalously cyclonic curvature in the flow tend to be associated with increased frequency of winter weather. This can even be seen in phase 7, which has increased frequency of winter weather events in the Deep South of the United States. This region is also located to the south of a significant troughing anomaly.

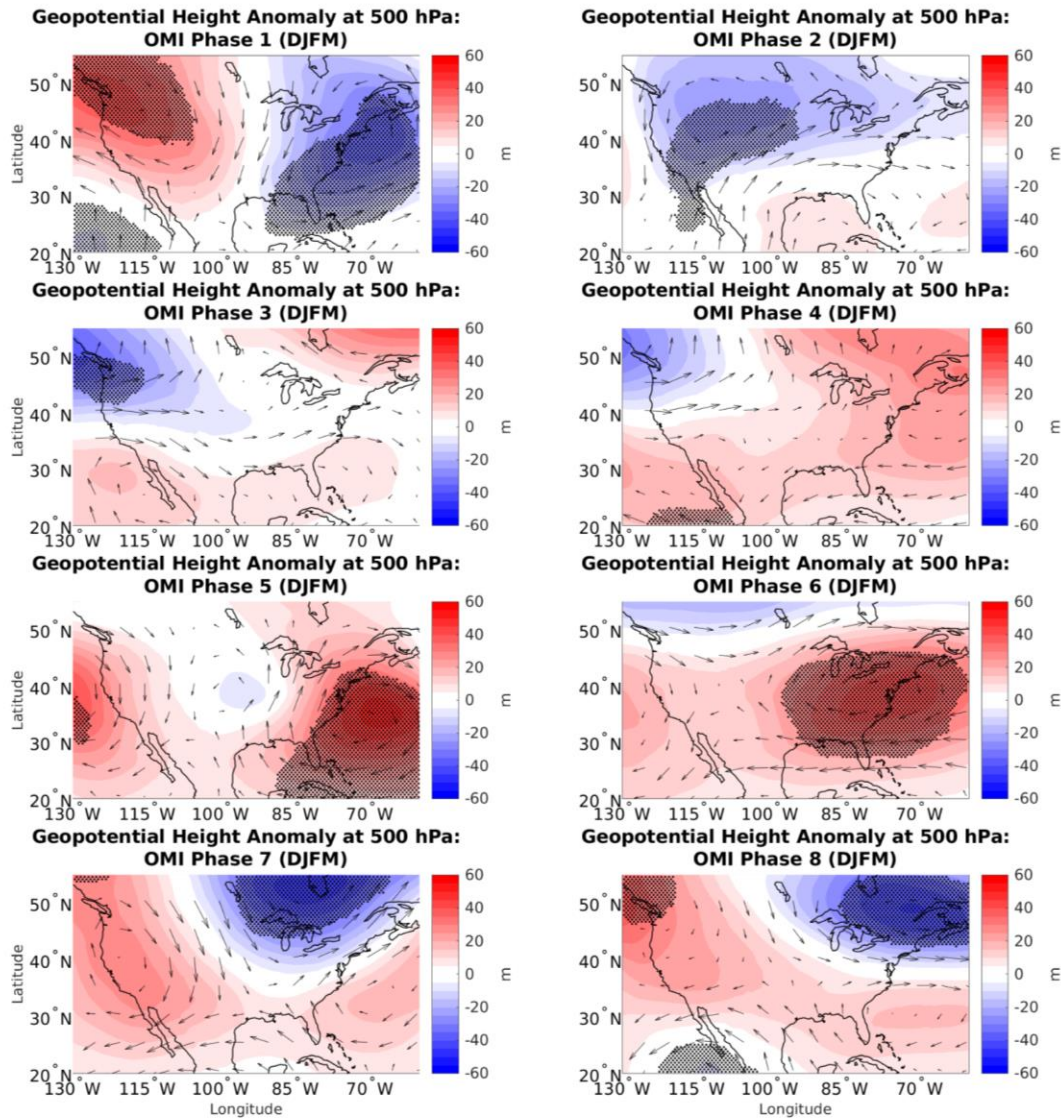


Figure 3.9: Geopotential height anomaly (m) at 500 hPa and wind anomaly (m s^{-1}) at 250 hPa.

The height anomalies can also be analyzed for the Northern Hemisphere as a whole (Figure 3.10). These anomalies are similar to those found by Zhou et al. (2011), with an area of low heights propagating east from the Aleutians in phase 1, to the Alaskan Panhandle by phase 3, Central Canada by phase 6, and the Northeast U.S. by phase 8. Some differences between the two results are likely due to difference in MJO index used (Zhou et al. used RMM) and the

difference in years used for the analysis. It is also possible to note blocking patterns similar to the NAO as noted in Cassou (2008). For example, the pattern in OMI phase 4 resembles the positive phase of the NAO, with lower geopotential heights near Iceland and higher heights near the Azores. The pattern in phases 7 and 8 resemble the negative phase of the NAO with higher height anomalies over Iceland and lower height anomalies to the south. This is one phase earlier than the connection between the NAO and surface air temperature anomalies. This could suggest that the MJO/NAO teleconnection influences the upper atmosphere before it influences the surface.

The upper height patterns also show connections between the MJO and PNA. OMI phase 3 approximates a negative PNA pattern, while phases 7 and 8 approximate a positive pattern. These results are similar to those of Riddle et al. (2013), who found a positive PNA pattern to be twice as likely as normal during and shortly after phase 8 of the MJO. However, they did not find the same results for increased frequency of a negative PNA pattern after phase 3 or 4 of the MJO (Riddle et al. 2013). A positive PNA is more likely to lead to above normal snowfall in the Eastern U.S., while it will lead to below normal snowfall in the Upper Midwest (Serreze et al. 1998). Phase 4, which produces heavy snow in the Northern Plains, also tends to result in a negative PNA-type pattern that is associated with heavy snowfall in that region. These teleconnection patterns hint at possible predictability for the MJO on winter weather events beyond 15 days. However, that is beyond the scope of this analysis.

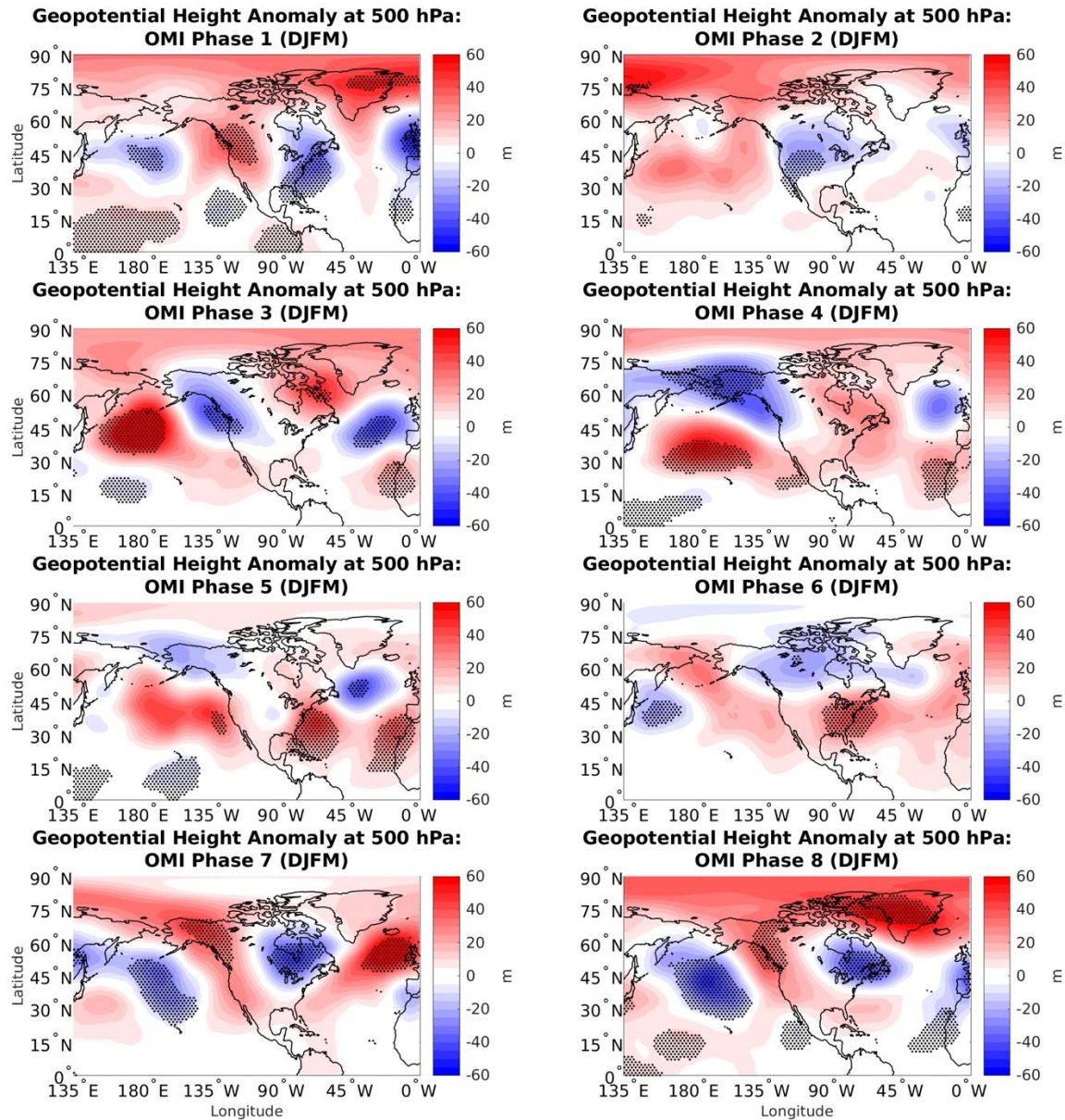


Figure 3.10: Geopotential height anomaly at 500 hPa for the Northern Hemisphere.

On days with winter weather events, there is a trough to the west and ridge to the east. For Northern Plains ice storms (Figure 3.11), the region is under a ridge, whereas for winter storms and heavy snow events, it is between the ridge and trough. The troughs generally appear to be slightly negatively tilted, especially for ice storm days. The details of these patterns do not

closely match any of the patterns based on OMI phase, but phases 3 and 4 appear to be the closest matches (Table 3.7). Phase 4 had a very high frequency of winter weather in the region, but phase 3 did not (Figure 2.8). So large correlations are sometimes associated with increased frequency of winter weather. OMI phases with frequent winter weather events often have a height pattern that is favorable for those sorts of events. However, an OMI phase that tends to have a favorable height pattern is not a guarantee of more frequent winter weather events.

In the Southern Great Plains (Figure 3.12), the centers of the troughs and ridges are located further south, and the tilt appears to be more neutral. Furthermore, the Southern Plains is on the gradient between higher and lower heights for ice storm days, whereas the Northern Plains is more completely within the region of higher heights. The pattern in the Southern Plains has similarities to OMI phases 2 or 3, except that those phases lack a ridge to the east. There is also a high correlation in height patterns between storm days and OMI phase 5 (Table 3.8), yet winter weather frequency ratios tend to be below normal in those regions (Figure 2.9). Phase 2 had a high frequency of winter weather in the region, while in phase 3 (Figure 2.9), the frequency ratios were closer to normal. This means that perhaps the trough in the west in phase 2 is more important than the ridge to the east in phase 5. Similar to the Northern Plains, phases with frequent winter weather events tend to have a more favorable height pattern, but a favorable height pattern is not a guarantee of frequent winter weather events.

The patterns in the Northeast (Figure 3.13) tend to be similar to those in the Northern Great Plains, with the ridges and troughs located in similar relative positions. The exceptions are for heavy snow days in the Northeast, where there is a more neutrally tilted trough, and the center of the low is shifted slightly further south. These patterns have similarities to OMI phases 2 or 7, where there is a trough to the west of the region. Phases 2 and 7 both have positive

correlations between the different regions for heavy snow and winter storm days (Table 3.9). However, the frequency ratio in both phases was near normal (Figures 2.3 and 2.4 b and g). Phases 1 and 8 had high spatial correlations for heavy snow days but not winter storm or ice storm days. Phase 1 had a high frequency ratio for heavy snow, but it was near 1 in phase 8. Therefore, in this case, the effects of the MJO on height patterns did not seem to be particularly related to the frequency of winter weather. In all situations, the flow pattern on days with severe winter weather is much more amplified than the average pattern in a given OMI phase. This is likely due in part to the fact that severe winter weather happens on only a few days in a given winter, so any given OMI phase will only have a small fraction of days with winter weather. And thus the more extreme days with severe winter weather will get smoothed out.

When considering lead times of geopotential height for Northern Plains storm days (not shown), it was found that the ridge and trough pattern was relatively transient (moving across the CONUS over a few days). In contrast, the height anomalies associated with the MJO remain relatively stationary over the course of a few days, as expected from intraseasonal anomalies. Given that the synoptic variability has a stronger impact on the occurrence of winter weather, a given phase of the MJO will not likely cause winter storms to develop unless favorable synoptic conditions are also present to develop winter storms. Therefore, we speculate that the MJO modulates winter weather events in part by generating intraseasonal atmospheric conditions that are more or less favorable for severe winter weather by causing patterns that are similar to the synoptic patterns associated with storm days. Whether these more favorable patterns actually result in winter weather is less likely to be affected by the MJO and more likely to be affected by other features not analyzed here. Further study is needed to determine why favorable patterns sometimes but not always lead to increased winter weather frequency.

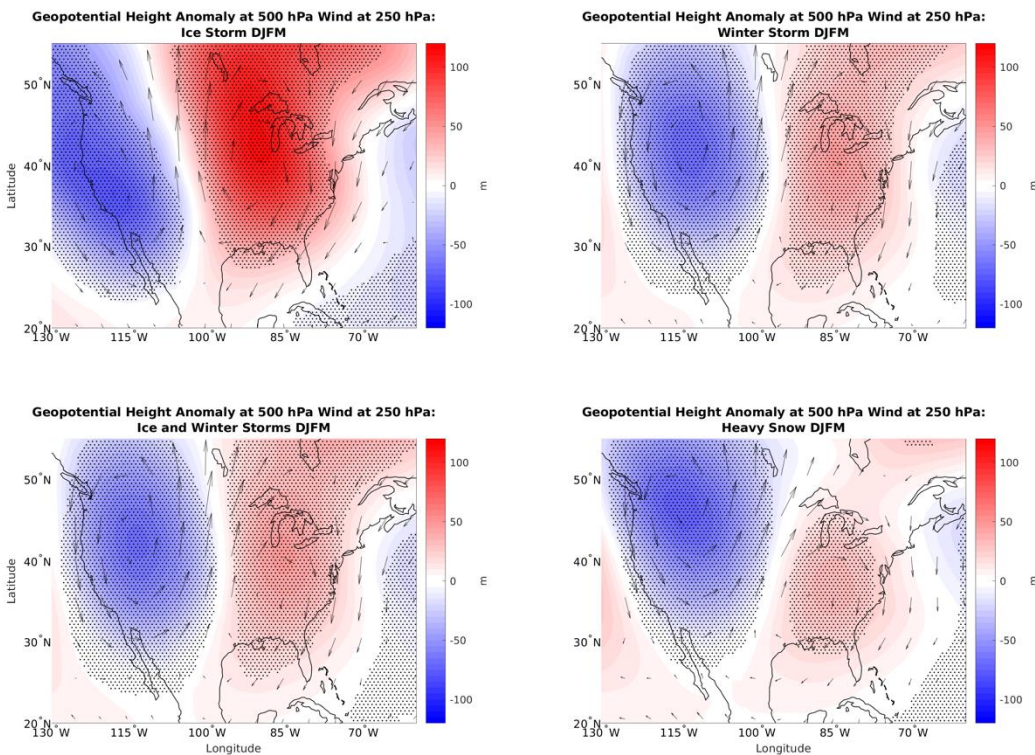


Figure 3.11: Geopotential height anomaly at 500 hPa and wind anomaly at 250 hPa associated with different types of winter weather events in the Northern Great Plains.

Table 3.7: Correlation between 500 hPa geopotential height anomalies on days with given storm type in the Northern Plains and OMI phase

OMI Phase	1	2	3	4	5	6	7	8
Heavy snow	-0.76	0.63	0.69	0.67	0.38	0.54	-0.38	-0.41
Winter storm	-0.76	0.41	0.54	0.56	0.23	0.40	-0.61	-0.54
Ice storm	-0.51	-0.19	0.32	0.42	-0.27	0.16	-0.84	-0.58

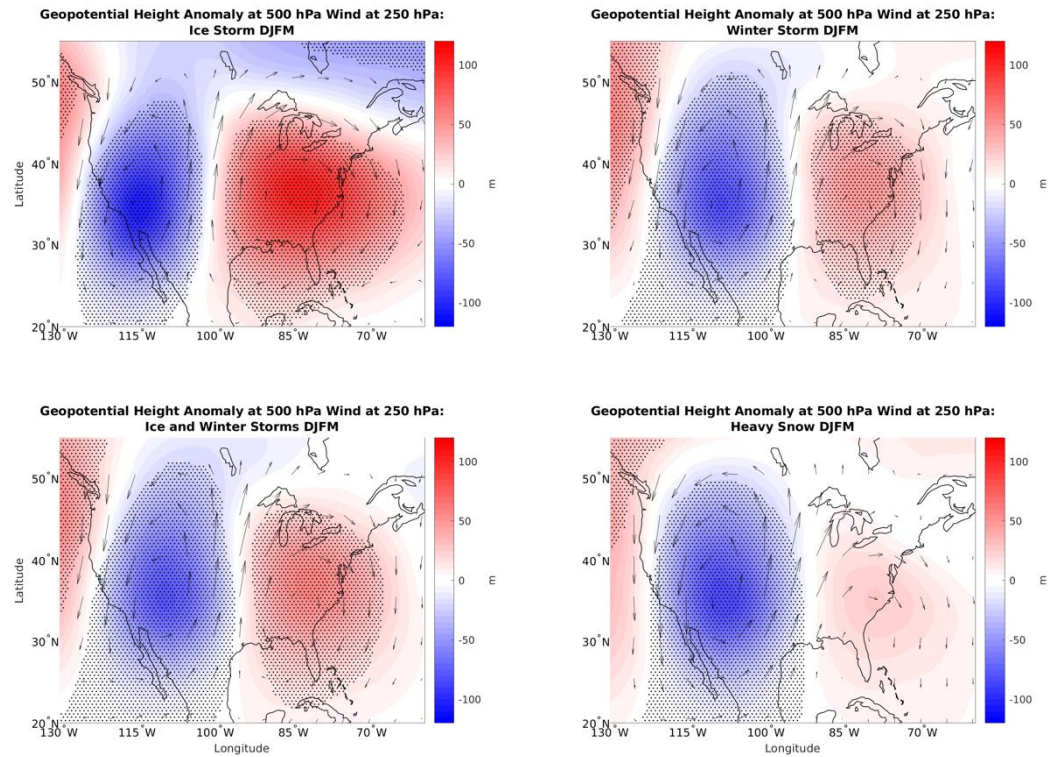


Figure 3.12: Same as Fig. 3.11 but for the Southern Great Plains.

Table 3.8: Correlation between 500 hPa geopotential height anomalies on days with given storm type in the Southern Plains and OMI phase

OMI Phase	1	2	3	4	5	6	7	8
Heavy snow	-0.45	0.36	0.10	0.08	0.48	0.15	-0.21	-0.16
Winter storm	-0.44	0.32	-0.02	0.02	0.47	0.32	-0.16	-0.10
Ice storm	-0.47	0.35	-0.11	0.03	0.35	0.59	-0.06	0.08

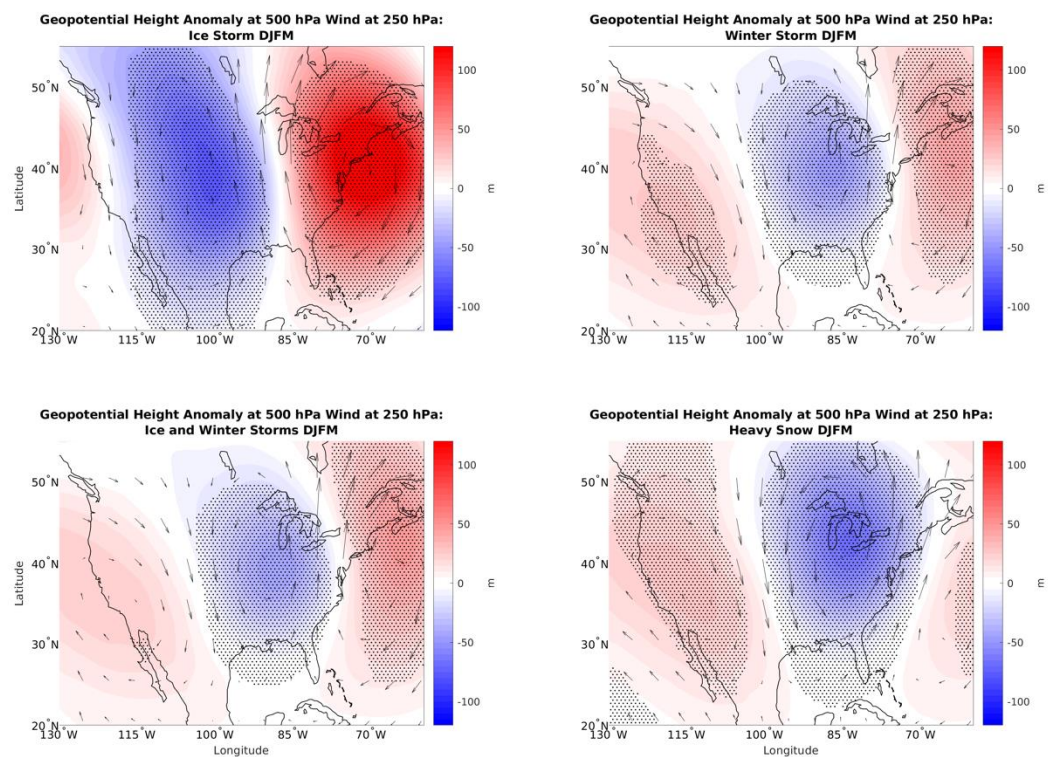


Figure 3.13: Same as Fig. 3.11 but for the Northeast.

Table 3.9: Correlation between 500 hPa geopotential height anomalies on days with given storm type in the Northeast and OMI phase

OMI Phase	1	2	3	4	5	6	7	8
Heavy snow	0.54	0.23	-0.16	-0.34	0.08	-0.35	0.76	0.55
Winter storm	0.01	0.26	0.17	0.15	0.44	-0.06	0.40	-0.01
Ice storm	-0.79	0.26	0.31	0.54	0.78	0.56	-0.25	-0.49

3.2.4. Specific Humidity Anomalies

Specific humidity anomalies at 700 hPa tend to have few significant values over the United States when they are analyzed by OMI phase (Figure 3.14). There are some drier than normal areas in the Southwest in phase 5 and some wetter than normal areas in phase 6. Phase 1 had some drier areas over the Northeast and Mid-Atlantic, in spite of those areas having increased frequency of winter weather events. That region did have cooler than normal temperatures during phase 1 (Figure 3.1), making temperature a more likely cause of increased winter weather events in that region. Phase 2 also had drier areas over the Northern Plains, and had some areas with above normal winter weather frequency ratios (Figure 2.4b).

When considering days and regions where winter weather events occur, specific humidity values tend to be higher. Furthermore, especially for winter storm and heavy snow events, there is moisture advection into the area. This is important for precipitation development. Given that specific humidity is the opposite sign in phase 1 as for winter weather event days in the Northeast (Figure 3.15), it appears that that is not a way that the MJO influences the frequency of winter weather events. This is also the case for phase 2 and winter weather in the Great Plains. However, the statistical correlations between specific humidity values on days with winter weather and OMI phases with frequent winter weather were largely positive. Visual inspection of the results suggests that much of this positive correlation is due to lower specific humidity anomalies in the West and higher values in the Atlantic in OMI phases 1 and 3.

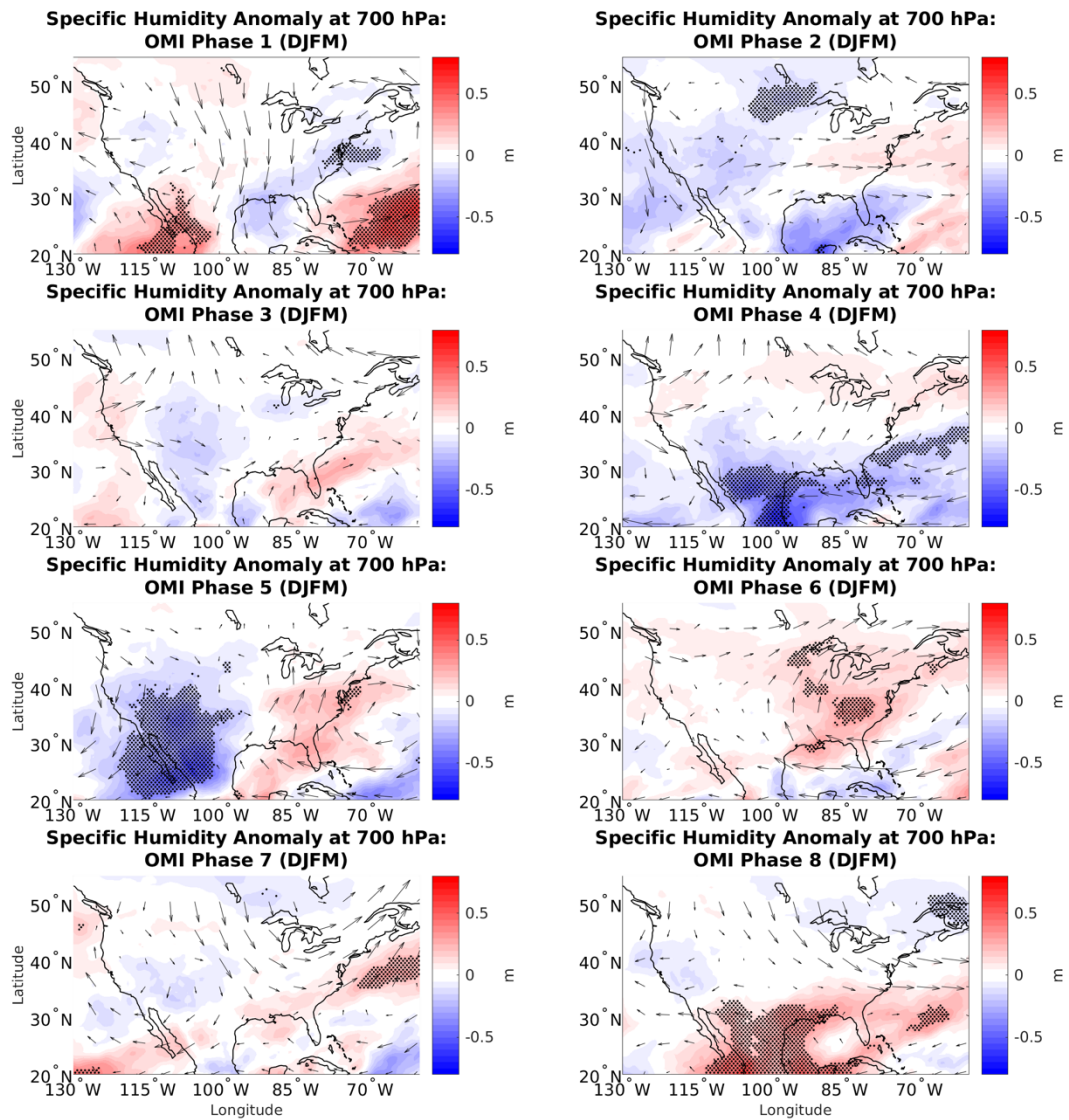


Figure 3.14: Specific humidity and wind anomalies at 700 hPa by OMI phase.

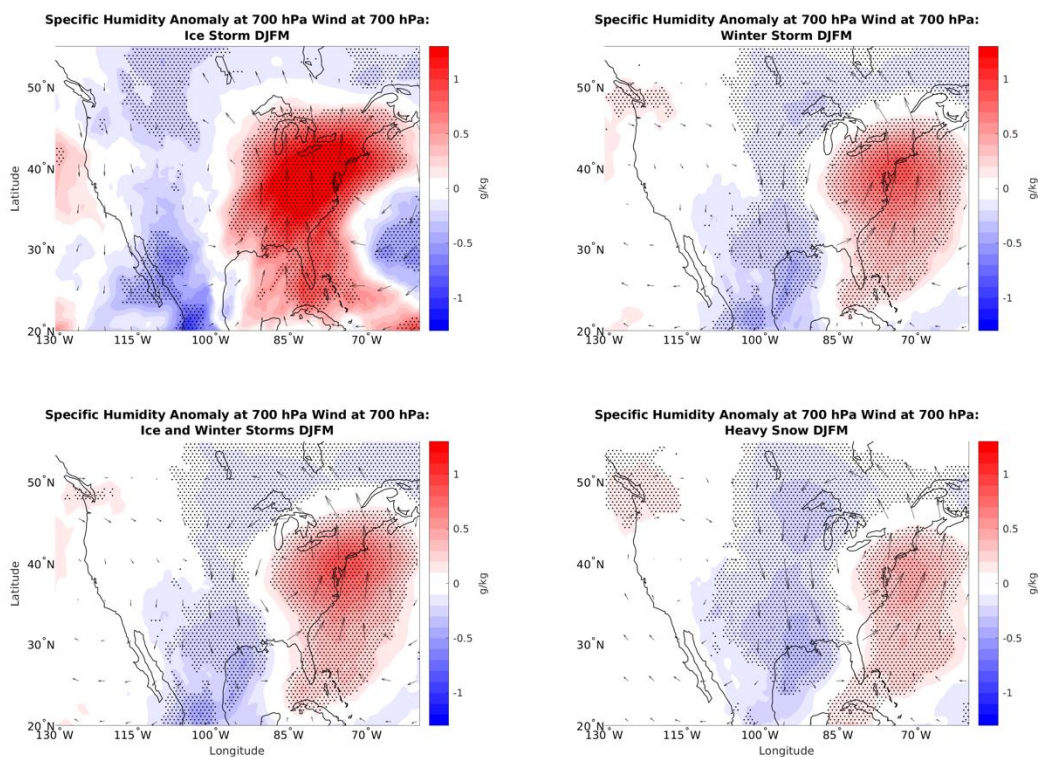


Figure 3.15: Specific humidity and wind anomalies at 700 hPa associated with different types of winter weather events in the Northeast.

Table 3.10: Correlation between 700 hPa specific humidity anomalies on days with given storm type in the Northeast and OMI phase

OMI Phase	1	2	3	4	5	6	7	8
Heavy snow	0.13	0.32	0.42	0.15	0.31	-0.12	0.39	-0.03
Winter storm	-0.13	0.37	0.41	0.25	0.48	0.17	0.37	-0.12
Ice storm	-0.34	0.19	0.18	0.15	0.61	0.46	0.16	-0.05

3.2.5. Large-Scale Synoptic Forcing of Ascent

The results indicate that the moisture and temperature anomalies alone do not necessarily explain why the MJO enhances winter weather over some particular regions. For example, the MJO did not lead to substantial cooling or moistening over the Northern Plains during phase 4. To determine if the MJO has an effect on large-scale vertical motion, we approximate the right-hand term of the QG- ω equation (Equation 3.1) to see if there are appreciable differences in quasi-geostrophic vertical motion forcing by OMI phase. Vertical motion forcing is computed at 500 hPa using the Trenberth form of the quasi-geostrophic omega (QG- ω) equation (Equation 3.1). This also requires the computation of the temperature gradient at that level.

$$\left(\nabla^2 p + \frac{f_0^2}{\sigma} \frac{\partial^2}{\partial p^2} \right) \omega = \frac{f_0}{\sigma} 2 \left(\frac{\partial \mathbf{v}_g}{\partial p} \cdot \nabla_p \zeta_g \right)$$

Equation 3.1: The QG- ω equation from Trenberth (1978).

In this case $\partial \mathbf{v}_g / \partial p$ is computed as the thermal wind based on the temperature gradient (Equations 3.2 and 3.3). The vorticity is computed from the wind at 500 hPa, with ζ_g approximated as ζ .

$$-\frac{\partial u_g}{\partial p} = -\frac{R}{f p} \left(\frac{\partial T}{\partial y} \right)_p$$

Equation 3.2: The thermal wind equation for zonal wind.

$$-\frac{\partial v_g}{\partial p} = \frac{R}{f p} \left(\frac{\partial T}{\partial x} \right)_p$$

Equation 3.3: The thermal wind equation for meridional wind.

We first analyze the vorticity advection (Figure 3.16) and thermal wind (not shown) components separately before analyzing them together (Figure 3.17). There were positive relative vorticity anomalies to the west of the Northern Great Plains in phase 4 (Figure 3.16). As

these vorticity anomalies were advected eastward, that could have led to forcing for rising motion. However, when the forcing term itself was computed, the results were very noisy (Figure 3.17). Further study and perhaps a different dataset would be needed to determine if vertical motion forcing could be shown to be affected by the MJO as a potential cause for its effects on winter weather event frequency.

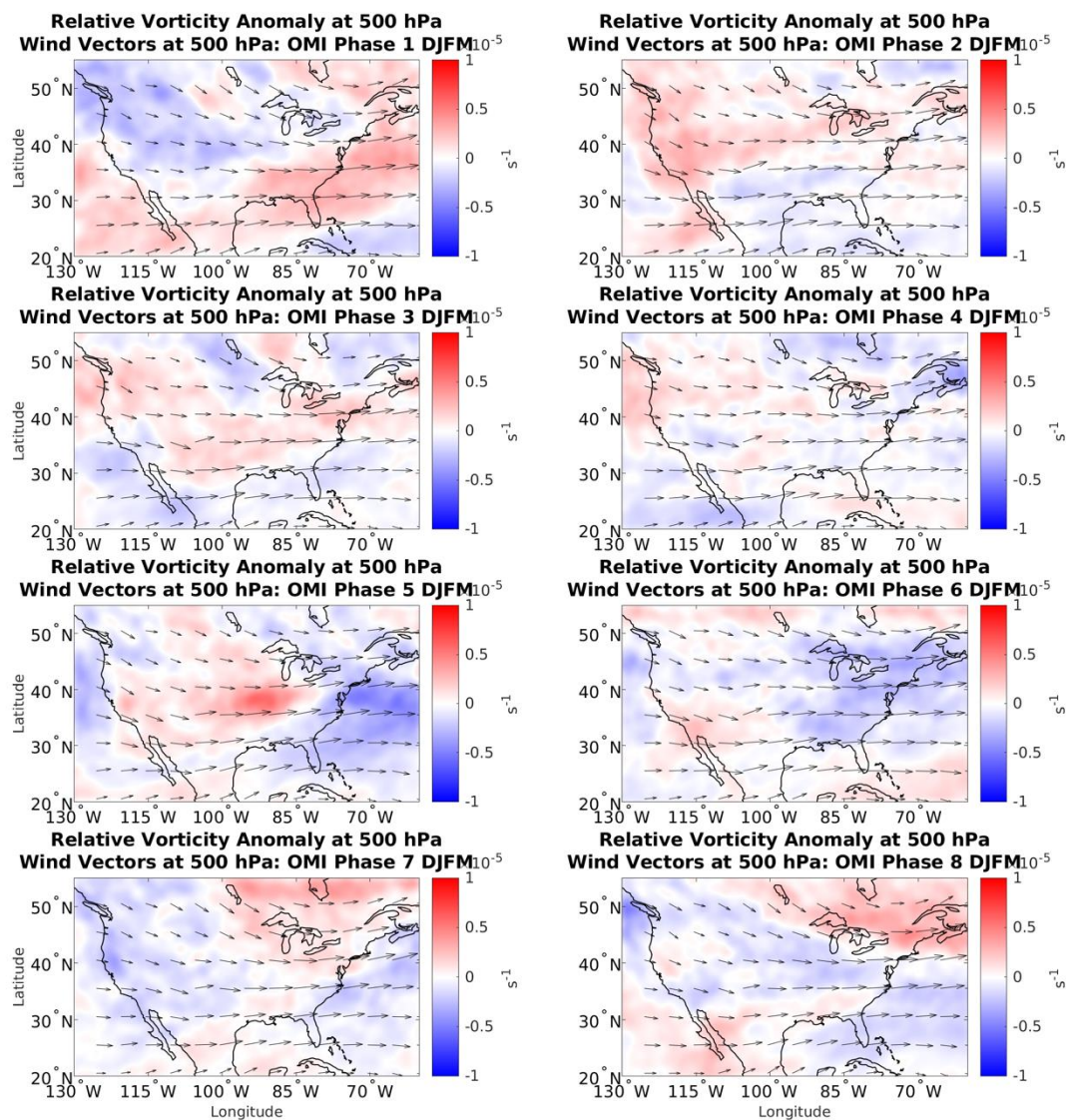


Figure 3.16: Relative vorticity anomalies and thermal wind vectors at 500 hPa by OMI phase.

Significance was not computed for these anomalies.

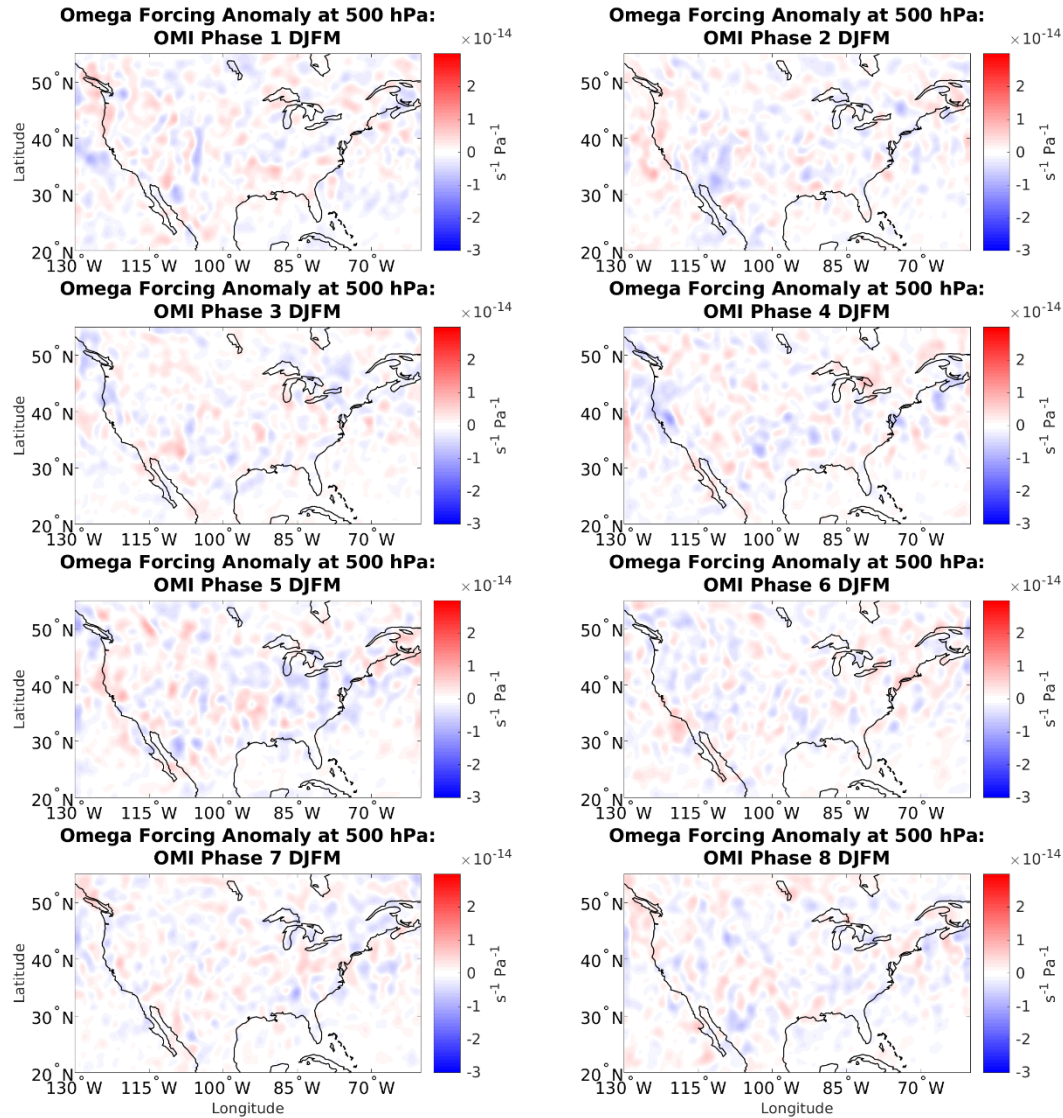


Figure 3.17: Vertical motion component anomalies at 500 hPa by OMI phase.

Overall, it appears that the MJO partially influences winter weather over the United States through changes in temperature in the lower atmosphere and geopotential height in the mid-troposphere, with the cooler temperatures and lower heights brought about by the MJO being favorable for winter weather. When looking at all three regions and all temperature and height combinations analyzed here, we find that the spatial correlations for phases with a significant increase in winter weather are almost always positive. When comparing OMI phase

and days with heavy snow, 8 out of 9 correlations are positive, when looking at winter storm days, all 9 are positive, and for ice storm days, 7 out of 9 correlations are positive. However, the OMI phases with the highest correlations did not always have frequency ratios that were as large. Therefore, other factors must be at play when analyzing how the MJO affects winter weather. Another area of MJO influence is in the circulation patterns at 850 hPa, where cyclonic circulation is favorable for winter storm development. However, connections between the MJO and specific humidity did not appear to cause changes in the frequency of winter weather over the US, and no connection was found between the MJO and vertical motion using the QG- ω equation.

4. Discussion and Conclusion

The MJO has significant impacts on the frequency of winter weather over the contiguous United States. Some major areas of increased frequency include phase 1 over the Northeast, phase 2 over the Southern Plains, phase 3 over the West, and phase 4 over the Northern Plains. Phases 5-7 did not have many areas of high frequency ratios. These results are true primarily for heavy snow and winter storm events. Ice storms also have an above normal occurrence over the Southern Plains during phase 2 and over the Northeast during phase 8. A handful of locations around the country had above normal frequency on days when there was little to no MJO convection. The changes in frequency by MJO phase can be seen both in results from the NCEI storm database and GHCN historical weather data. It can be seen when either OMI or RMM is used to determine the phase of the MJO. These changes in frequency can be seen as far as 15 days after a given phase of the MJO, suggesting potential uses for S2S forecasting. The changes in frequency ratio as lag increases occur at a similar rate to the duration of each MJO phase, which provides further evidence of an association with the MJO. These changes appear to be more appreciable in the northern two-thirds of the country, where severe winter weather is more frequent.

The MJO appears to influence the frequency of winter weather events in part by changing the temperature, flow, and height patterns due to Rossby wave propagations from the tropics. Temperature and height anomalies are most appreciable during phases 1 and 2 over the Northeast and Southern Plains. These patterns were often similar to patterns found on days with winter weather reports over a given region. However, the patterns associated with each MJO phase were generally less extreme than the patterns associated with winter weather events. Also, temperature and height anomalies during some MJO phases had high spatial correlations with winter weather

days, but did not have high frequency ratios. The increase in frequency ratio for winter weather in the Northern Great Plains during phase 4 was not fully explained by this analysis. However, OMI phase 4 was similar to the negative phase of the PNA, which is associated with increased snowfall in the region. So, the MJO/PNA teleconnection would be a promising area of future research to discern the method of MJO impact on snowfall in the Northern Plains. The impacts the MJO has on humidity had relatively little influence on the frequency of winter weather. There were difficulties in determining if the MJO had any significant impact on the synoptic forcing of vertical motion over the United States.

Some areas of future research include examining how combinations of the MJO, NAO, and PNA influence winter weather over the United States. Analyzing automated surface observing system (ASOS) freezing rain reports to compare with NCEI ice storm reports is another area that may provide more data when analyzing the impact of the MJO on ice storms. Inversions were not calculated directly, but that could be a future variable to analyze. Blizzards are another category in NCEI that could be analyzed to determine how the MJO affects the frequency of that weather phenomenon. Another potential future research avenue is expanding the forecast window to look at how the MJO affects the frequency of winter weather events in the 20-30-day time period. An analysis of lagged height and wind values could also be conducted to determine more specifically how the MJO signal propagates to the United States. Thus, there is much left to discover as we look into the many ways the MJO influences winter weather over the contiguous United States, and its utility on the S2S time scale.

5. References

- Black, R.E., 1971: A Synoptic Climatology of Blizzards on the North-Central Plains of the United States. NOAA Technical Memorandum NWS CR-39, 47 pp.
- Cassou, C., 2008: Intraseasonal interaction between the Madden-Julian Oscillation and the North Atlantic Oscillation. *Nat.*, **455**, 523-527, <https://doi.org/10.1175/MWR-D-15-0434.1>.
- Changnon, S.A. and T.R. Karl, 2003: Temporal and Spatial Variations of Freezing Rain in the Contiguous United States: 1948-2000. *J. Appl. Meteor. Climatol.*, **42**, 1302-1315, [https://doi.org/10.1175/1520-0450\(2003\)042<1302:TASVOF>2.0.CO;2](https://doi.org/10.1175/1520-0450(2003)042<1302:TASVOF>2.0.CO;2).
- Changnon, S.A., 2006: Frequency Distributions of Heavy Snowfall from Snowstorms in the United States. *J. Hydrol. Eng.* **11**, 427-431, [https://doi.org/10.1061/\(ASCE\)1084-0699\(2006\)11:5\(427\)](https://doi.org/10.1061/(ASCE)1084-0699(2006)11:5(427)).
- Cohen, J., K. Pfeiffer, and J.A. Francis, 2018: Warm Arctic episodes linked with increased frequency of extreme winter weather in the United States. *Nat. Comm.*, **9**, 869, 1-12, <https://doi.org/10.1038/s41467-018-02992-9>.
- Gottschalk, J., 2014: What is the MJO, and why do we care? NOAA Climate.gov. Accessed 5 April 2022, <https://www.climate.gov/news-features/blogs/enso/what-mjo-and-why-do-we-care>.
- Greatbatch, R.J., 2000: The North Atlantic Oscillation. *Stochastic Environ. Res. Risk Assess.*, **14**, 213-242, <https://doi.org/10.1007/s004770000047>.
- Green, M.R. and J.C. Furtado, 2019: Evaluating the Joint Influence of the Madden-Julian Oscillation and the Stratospheric Polar Vortex on Weather Patterns in the Northern Hemisphere. *JGR Atmospheres*, **124**, 11693-11709, <https://doi.org/10.1029/2019JD030771>.
- Grundstein, A., 2003: A Synoptic-Scale Climate Analysis of Anomalous Snow Water Equivalent over the Northern Great Plains of the USA, *Int. J. Climatol.*, **23**, 871-886, <https://doi.org/10.1002/joc.908>.
- Hartley, S. and M.J. Keables, 1998: Synoptic Associations of Winter Climate and Snowfall Variability in New England, USA, 1950-1992, *Int. J. Climatol.*, **18**, 281-298, [https://doi.org/10.1002/\(SICI\)1097-0088\(19980315\)18:3<281::AID-JOC245>3.0.CO;2-F](https://doi.org/10.1002/(SICI)1097-0088(19980315)18:3<281::AID-JOC245>3.0.CO;2-F).

- Hersbach, H., and Coauthors, 2020: The ERA5 global reanalysis. *Quart. J. Roy. Meteor. Soc.*, **146**, 1999-2049, <https://doi.org/10.1002/qj.3803>.
- Huguley, D., 2009: APRS NWS Weather Info, 1. APRS, accessed 14 July 2021, <http://www.aprs-is.net/WX/NWSZones.aspx>.
- Jiang, X., Á.F. Adames, D. Kim, E.D. Maloney, H. Lin, H. Kim, C. Zhang, C.A. DeMott, and N.P. Klingaman, 2020: Fifty Years of Research on the Madden-Julian Oscillation: Recent Progress, Challenges, and Perspectives. *JGR Atmospheres*, **125**, 17, 1-64, <https://doi.org/10.1029/2019JD030911>.
- Kiladis, G.N., J. Dias, K.H. Straub, M.C. Wheeler, S.N. Tulich, K. Kikuchi, K.M. Weickmann, and M.J. Ventrice, 2014: A Comparison of OLR and Circulation-Based Indices for Tracking the MJO. *Mon. Wea. Rev.*, **142**, 1697-1715, <https://doi.org/10.1175/MWR-D-13-00301.1>.
- Klotzbach, P.J., E.C.J. Oliver, R.D. Leeper, and C.J. Schreck III, 2016: The Relationship between the Madden-Julian Oscillation (MJO) and Southeastern New England Snowfall. *Mon. Wea. Rev.*, **144**, 1355-1362, <https://doi.org/10.1175/MWR-D-15-0434.1>.
- Lin, H., G. Brunet, and J. Derome, 2009: An Observed Connection between the North Atlantic Oscillation and the Madden-Julian Oscillation. *J. Climate*, **22**, 364-380, <https://doi.org/10.1175/2008JCLI2515.1>.
- Madden, R.A. and P.R. Julian, 1971: Detection of a 40-50 Day Oscillation in the Zonal Wind in the Tropical Pacific. *J. Atmospheric Sci.*, **28**, 702-708, [https://doi.org/10.1175/1520-0469\(1971\)028<0702:DOADOI>2.0.CO;2](https://doi.org/10.1175/1520-0469(1971)028<0702:DOADOI>2.0.CO;2).
- Matsueda, S. and Y. Takaya, 2015: The Global Influence of the Madden-Julian Oscillation on Extreme Temperature Events. *J. Climate*, **28**, 4141-4151, <https://doi.org/10.1175/JCLI-D-14-00625.1>.
- McCray, C.D., E.H. Atallah, J.R. Gyakum, 2019: Long-Duration Freezing Rain Events over North America: Regional Climatology and Thermodynamic Evolution. *Wea. Forecasting*, **34**, 665-681, <https://doi.org/10.1175/WAF-D-18-0154.1>.

- Moon, J.-Y., B. Wang, and K.-J. Ha, 2012: MJO Modulation on 2009/10 Winter Snowstorms in the United States, *J. Climate*, **25**, 978-991, <https://journals.ametsoc.org/view/journals/clim/25/3/jcli-d-11-00033.1.xml>.
- Mullens, E.D., L.M. Leslie, and P.J. Lamb, 2016: Synoptic Pattern Analysis and Climatology of Ice and Snowstorms in the Southern Great Plains, 1993-2011. *Wea. Forecasting*, **31**, 1109-1136, <https://doi.org/10.1175/WAF-D-15-0172.1>.
- NCEI, 2021a: Storm Data, NCEI. Accessed 22 January 2021. <https://www.ncdc.noaa.gov/stormevents/>.
- NCEI, 2021b: Global Historical Climatology Network – Daily, Version 3. NCEI. Accessed 26 June 2021, <https://www1.ncdc.noaa.gov/pub/data/ghcn/daily/all/>.
- NCEI, 2022: Global Historical Climatology Network daily (GHCNd). NCEI. Accessed 6 June 2022, <https://www.ncei.noaa.gov/products/land-based-station/global-historical-climatology-network-daily>.
- Riddle, E.E., M.B. Stoner, N.C. Johnson, M.L. L’Heureux, D.C. Collins, S.B. Feldstein, 2013. *Climate Dyn.*, **40**, 1749-1766, <https://doi.org/10.1007/s00382-012-1493-y>.
- Sardeshmukh, P.D. and B.J. Hoskins, 1988: The Generation of Global Rotational Flow by Steady Idealized Tropical Divergence. *J. Atmospheric Sci.*, **45**, 1228-1251, [https://doi.org/10.1175/1520-0469\(1988\)045<1228:TGOGRF>2.0.CO;2](https://doi.org/10.1175/1520-0469(1988)045<1228:TGOGRF>2.0.CO;2).
- Serreze, M.C., M.P. Clark, D.L. McGinnis, D.A. Robinson, 1998: Characteristics of Snowfall over the Eastern Half of the United States and Relationships with Principal Modes of Low-Frequency Atmospheric Variability. *J. Climate*, **11**, 234-250, [https://doi.org/10.1175/1520-0442\(1998\)011<0234:COSOTE>2.0.CO;2](https://doi.org/10.1175/1520-0442(1998)011<0234:COSOTE>2.0.CO;2).
- Straub, K.H., 2013: MJO Initiation in the Real-Time Multivariate MJO Index, *J. Climate*, **26**, 1130-1151, <https://doi.org/10.1175/JCLI-D-12-00074.1>.
- Trenberth, K.E., 1978: On the Interpretation of the Diagnostic Quasi-Geostrophic Omega Equation. *Mon. Wea. Rev.*, **106**, 131-137.

- Tseng, K.-C., E.A. Barnes, and E.D. Maloney, 2017: Prediction of the Midlatitude Response to Strong Madden-Julian Oscillation Events on S2S Time Scales. *Geophys. Res. Lett.*, **45**, 463-470, <https://doi.org/10.1002/2017GL075734>.
- Vecchi, G.A. and N.A. Bond, 2004: The Madden-Julian Oscillation (MJO) and northern high latitude wintertime surface air temperatures. *Geophys. Res. Lett.*, **31**, 4, 1-4, <https://doi.org/10.1029/2003GL018645>.
- Wallace, J.M. and D.S. Gutzler, 1981: Teleconnections in the Geopotential Height Field during the Northern Hemisphere Winter. *Mon. Wea. Rev.*, **109**, 784-812, [https://doi.org/10.1175/1520-0493\(1981\)109<0784:TITGHF>2.0.CO;2](https://doi.org/10.1175/1520-0493(1981)109<0784:TITGHF>2.0.CO;2).
- Wang, B. and X. Xie, 1997: A Model for the Boreal Summer Intraseasonal Oscillation. *J. Atmospheric Sci.*, **54**, 72-86, [https://doi.org/10.1175/1520-0469\(1997\)054<0072:AMFTBS>2.0.CO;2](https://doi.org/10.1175/1520-0469(1997)054<0072:AMFTBS>2.0.CO;2).
- Wheeler, M.C. and H.H. Hendon, 2004: An All-Season Real-Time Multivariate MJO Index: Development of an Index for Monitoring and Prediction. *Mon. Wea. Rev.*, **132**, 1917-1932, [https://doi.org/10.1175/1520-0493\(2004\)132<1917:AARMMI>2.0.CO;2](https://doi.org/10.1175/1520-0493(2004)132<1917:AARMMI>2.0.CO;2).
- Wiley, J. and A. Mercer, 2021: Synoptic Climatology of Lake-Effect Snow Events off the Western Great Lakes. *Climate.*, **9**, 43, 1-21, <https://doi.org/10.3390/cli9030043>.
- Zhang, F., Y.Q. Sun, L. Magnusson, R. Buizza, S. Lin, J. Chen, and K. Emanuel, 2019: What Is the Predictability Limit of Midlatitude Weather? *J. Atmospheric Sci.*, **76**, 1077-1091, <https://doi.org/10.1175/JAS-D-18-0269.1>.
- Zhou, S., M. L'Heureux, S. Weaver, and A. Kumar, 2012: A composite study of the MJO influence on the surface air temperature and precipitation over the Continental United States. *Climate Dyn.*, **38**, 1459-1471, <https://doi.org/10.1007/s00382-011-1001-9>.
- Zhou, Y., K.R. Thompson, and Y. Lu, 2011: Mapping the Relationship between Northern Hemisphere Winter Surface Air Temperature and the Madden-Julian Oscillation. *Mon. Wea. Rev.*, **139**, 2439-2454, <https://doi.org/10.1175/2011MWR3587.1>.

Zielinski, G.A., 2002: A Classification Scheme for Winter Storms in the Eastern and Central United States with an Emphasis on Nor'easters. *Bull. Amer. Meteor. Soc.*, **83**, 37-52,
[https://doi.org/10.1175/1520-0477\(2002\)083<0037:ACSFWS>2.3.CO;2](https://doi.org/10.1175/1520-0477(2002)083<0037:ACSFWS>2.3.CO;2).